DERIVATIVE-FREE KALMAN FILTER-BASED CONTROL OF NONLINEAR SYSTEMS WITH APPLICATION TO TRANSFEMORAL PROSTHESES

Seyed M. Moosavi

Bachelor of Science in Electrical Engineering

Shiraz University

September 2008

submitted in partial fulfillment of requirements for the degree

MASTER OF SCIENCE IN ELECTRICAL ENGINEERING

at the

CLEVELAND STATE UNIVERSITY

August 2017

We hereby approve this thesis for

Seyed M. Moosavi

Candidate for the Master of Science in Electrical Engineering degree for the

Department of Electrical Engineering and Computer Science

and the CLEVELAND STATE UNIVERSITY

College of Graduate Studies

Thesis Chairperson, Committee member name

Department & Date

Thesis Committee Member, Committee member name

Department & Date

Thesis Committee Member, Committee member name

Department & Date

Student's Date of Defense: July 20, 2017

ACKNOWLEDGMENTS

This is a different kind of acknowledgment because it is written by me, Prof. Dan Simon, Seyed's research advisor. Seyed finished his thesis in May 2017. The only thing remaining was the technical editing of his thesis and his oral defense. Then, in June, we received the devastating news that Seyed suddenly and unexpectedly passed away. Since his thesis was essentially complete, we were able to finish editing his thesis in July and August, and he was able to graduate posthumously in August with his master's degree in electrical engineering.

I am thankful for several individuals who supported Seyed's graduation despite his untimely passing: Prof. Anette Karlsson, the Dean of the College of Engineering; Prof. Chansu Yu, the Chair of the Department of Electrical Engineering and Computer Science; Ms. Melanie Caves, secretary of the Department; Mr. John Berzanske, master's student, whose technical editing was instrumental in the completion of this thesis; Mr. Seyed Fakoorian and Mr. Mohamed Abdelhady, doctoral students, who provided valuable input and corrections to the appendix; and Prof. Antonie van den Bogert and Prof. Hanz Richter, Seyed's thesis committee members, who provided several important corrections to the final version of the thesis and were very supportive throughout this process.

Seyed was extremely intelligent, likable, friendly, perceptive, helpful, and persistent. His loss is a terrible blow to the CSU community, his friends, his family, the engineering profession, and the human race. I dedicate this thesis to the fond memory of Seyed, and to his family. You have my deepest and most sincere condolences. I will never forget Seyed.

DERIVATIVE-FREE KALMAN FILTER-BASED CONTROL OF NONLINEAR SYSTEMS WITH APPLICATION TO TRANSFEMORAL PROSTHESES

Seyed M. Moosavi

ABSTRACT

Derivative-free Kalman filtering (DKF) for estimation-based control of a special class of nonlinear systems is presented. The method includes a standard Kalman filter for the estimation of both states and unknown inputs, and a nonlinear system that is transformed to controllable canonical state space form through feedback linearization (FL). A direct current (DC) motor with an input torque that is a nonlinear function of the state is considered as a case study for a nonlinear single-input-single-output (SISO) system. A three degree-of-freedom (DOF) robot / prosthesis system, which includes a robot that emulates human hip and thigh motion and a powered (active) transfemoral prosthesis disturbed by ground reaction force (GRF), is considered as a case study for a nonlinear multi-input-multi-output (MIMO) system. A PD/PI control term is used to compensate for the unknown GRF.

Simulation results show that FL can compensate for the system's nonlinearities through a virtual control term, in contrast to Taylor series linearization, which is only a first-order linearization method. FL improves estimation performance relative to the extended Kalman filter, and in some cases improves the initial condition region of attraction as well.

A stability analysis of the DKF-based control method, considering both estimation and unknown input compensation, is also presented. The error dynamics are studied in both frequency and time domains. The derivative of the unknown input plays a key role in the error dynamics and is the primary limiting factor of the closed-loop estimation-based control system stability. It is shown that in realistic systems the derivative of the unknown input is the primary determinant of the region of convergence. It is shown that the tracking error asymptotically converges to the derivative of the unknown input.

TABLE OF CONTENTS

LIST OF FIGURES

LIST OF TABLES

CHAPTER I

INTRODUCTION

Prosthesis technology has a long history, beginning with simple devices comprised mostly of wood and iron, and progressing to today's sophisticated high-technology robotic devices. Throughout this long history, many new designs and developments have emerged, and many other methods have become obsolete. Egyptians were likely the first to use prosthetic technology, as demonstrated by a recently discovered prosthetic toe from an Egyptian mummy [46].

Amputations are performed on various parts of the body. Transtibial, or below-knee, amputation is the most common, comprising 54% of all amputations. Transfemoral, or above-knee, amputation is the second most common, accounting for 33% of all amputations. Other amputations, such as upper limb, foot, and hip and knee disarticulations, constitute 7%, 3%, 2% and 1% respectively [48]. The most common reason for lower limb aputation is vascular disease, and more precisely diabetes. As of 2014, two-million people in the United States lived with limb loss, and this number increases by 185,000 annually [71]. There are currently more than 400,000 transfemoral amputees in the United States [1].

One of the greatest challenges for a leg amputee is the amount of biomechanical energy needed for walking. Transfemoral amputees expend over 60% more energy while walking than an able-bodied person [12]. This indicates that an amputee needs a well-

designed prosthetic leg to increase quality of life. Reducing prosthesis weight by using light components can make a significant improvement in amputees' lives. Another need for prosthetic legs is reliable and stable control laws. Estimation-based robotic technology allows for the removal of bulky load cells and other heavy sensors in prostheses. Although these improvements may not result in a gait that is equivalent to that of able-bodied persons, they can help provide a better approximation of normal gait.

1.1 Motivation

Transfemoral prosthesis design and development originally included only passive (also called reactive) devices, meaning that the leg was completely mechanical and did not include any electrical components [38], [32]. As mentioned earlier, the main problem with this type of prosthesis is the large amount of energy that an amputee has to expend during walking, in comparison with able-bodied persons [3], [12]. To address this problem, researchers have used electric power and microelectronic devices in prosthesis designs, leading to the development of semi-active prosthetic knees [56]. Semi-active prostheses have shown better and more reliable walking for amputees in terms of energy usage and adaptability to sloped surfaces [14], [28]. Semi-active prostheses are actuated through a mechanical damper or a hydraulic actuator, and the microelectronic device is used for control and measurement. The combination of microelectronics and mechanical components comprise the prosthetic system.

Active prostheses are the most recent generation of prosthesis technology. These prostheses use servo-motors in the knee or ankle in addition to microprocessor-based control. Highly efficient brushless DC motors have been used to generate high torque with fast response, which can improve walking for amputees. Many researchers are working are studying these ideas [4], [2], [41], [24], [26], [39], [62], [65], [69].

In this thesis, an active or powered transfemoral prosthetic leg is considered,

which is connected to a robotic hip / thigh emulator. The combination of the prosthesis and robot comprise three degrees of freedom: vertical hip displacement, thigh angle, and knee angle [17]. Much research has been done at Cleveland State University to obtain effective prosthesis control and estimation [5], [6], [16], [42], [50]. Research at CSU has included ground reaction force (GRF) estimation for prostheses so that bulky, expensive, and failure-prone load cells can be removed from the system [19], [51]. Several nonlinear estimators have been used for this purpose, such as the extended Kalman filter (EKF) and the unscented Kalman filter (UKF). In all of this previous research, the controllers and estimators have heavily relied on the known GRF model.

The goal of this thesis is to obtain effective GRF estimation and prosthesis control while considering the GRF as an unknown input, meaning that there is no information available about its dynamics. In previous research, inaccurate GRF modeling could cause undesirable performance in both the controller and the estimator. This thesis proposes a model-free supervisory control term, or GRF estimator, to reduce the dependence of both the controller and the filter on the unknown GRF. Previous research has shown that nonlinear GRF filters are very dependent on initial conditions, and slight changes in initial conditions can cause instability or poor performance. Also, extended Kalman filters (EKFs) are highly dependent on the system gradient, a dependence that can cause cumulative estimation errors and closed-loop instability [8], [18], [52], [57].

In this thesis, the system model is first transformed using feedback linearization (FL) to controllable canonical form. This transformation, unlike the EKF, does not ignore high-order nonlinear dynamics. The state of the linearized system dynamics is then estimated with a linear Kalman filter rather than an extended Kalman filter.

1.2 Literature Review

1.2.1 Transfemoral Leg Prostheses

The design and development of transfemoral leg prostheses has received considerable attention due to the increasing number of above-knee amputees [2], [41], [25], [28], [39], [65], [68], [70]. Recent advances in microelectronics and robotic technologies have led to new powered prosthetic leg technology. Transfemoral amputees who use powered (active) prosthetic legs expend less energy during walking compared with those who use passive prostheses, since powered prostheses can generate net power at the joints [63].

Test robots for transfemoral prostheses can emulate human walking in the sagittal plane [50], [51]. These test robots use nonlinear control and are connected to a prosthetic leg. Recent approaches to the control of a three degree-of-freedom robot / prosthesis system include passivity-based robust control [5], robust adaptive impedance control [50], hybrid control [16], and robust composite adaptive impedance control [6]. These methods have good tracking performance in the presence of parametric uncertainties and ground reaction force (GRF) disturbances. However, GRF in that research is assumed to have known dynamic properties and known bounds. Thus, besides the computational complexity of these control methods, tracking performance may degrade if the system is disturbed by unmodeled inputs.

1.2.2 Unknown-Input Estimation

As mentioned earlier, a wide variety of techniques have been employed to provide accurate and reliable tracking for robot / prosthesis systems. However, most of those methods depend on a good mathematical model for the GRF. In real-world applications it is possible for the robot / prosthesis to be perturbed by unknown inputs or disturbances with unknown dynamics. This problem is not specific to this particular robotic system. A broad range

of applications have reported similar problems due to unknown inputs, including real-time estimation of mean precipitation [35], nonparametric input estimation in physiological systems [45], fault diagnosis in dynamic systems [47], and estimation of cutting force exerted by tools [13]. Research in this area has focused on state and input estimation of linear systems subject to disturbances with known dynamics or known bounds [54].

Several minimum variance filters have been introduced for state estimation in the presence of unknown inputs [11], [15], [35]. However, the estimation of unknown inputs remains a major challenge. Inferring information about unknown inputs has a major effect on improved state estimation and results in more effective control [22] , [66]. However, the literature still lacks a general approach to this problem.

Recent research has attempted to address this issue through the simultaneous minimum variance estimation of both states and unknown inputs in linear, time-varying, continuous-time, stochastic systems [67]. The authors proposed two different filters for two different cases. The first filter was constructed under the assumption that certain additional information about the states was available. Although the method appears to be effective in theory and simulation, the additional required information is not realistic in practical applications. The second method addressed the drawbacks of the first method in that it assumed no additional information about the states. However, it was assumed that the unknown input is sufficiently smooth with bounded derivatives. This is a common assumption because if the unknown input is not sufficiently smooth or does not have bounded derivatives, there can be no guarantee of asymptotic stability. A separation principle was discussed for both proposed filters in terms of closed-loop control, meaning that the control feedback gain is independent of the filter or observer gain. For most linear closed-loop control systems this separation principle arises from the unique properties of linear systems theory.

Two categories of unknown-input estimation have received signficant attention: unmodeled dynamics, which can be viewed as the result of small perturbations on the

system parameters [27], [37]; and unknown external inputs, which have no contribution to the model dynamics [33], [64].

The disturbance observer (DOB) [29], [55], [64] is a common unknown-input estimator for linear systems, largely relying on a transfer function approach rather than state space. The unknown-input observer (UIO) was developed [30] after the DOB, and while including many of the properties of the DOB, it was based on a state space approach rather than a transfer function approach. A key property of the UIO is that it is able to estimate both states and unknown inputs. As with other estimators, the UIO was introduced for linear systems [7], [23] but later was extended to nonlinear systems [10], [44].

The perturbation observer (POB) is another unknown input estimator that has similarities to the DOB. The POB has the advantage of being able to handle both unknown inputs and unmodeled dynamics [36]. The extended state observer (ESO) [9] estimates unmodeled dynamics for the purpose of reducing control system dependence on unmodeled dynamics. The ESO is relatively simple in comparison with the DOB and the UIO. The ESO has been widely applied [20] to systems such as voltage regulation in DC-DC converters [61], high torque servo-motion control [21], and web tension regulation [31].

1.2.3 Derivative-Free Kalman Filtering

The derivative-free Kalman filter (DKF) was introduced for estimation-based control of a certain class of input-output linearizable nonlinear systems [52]. First, the nonlinear system was linearized and controlled by exact feedback linearization. Next, the standard, linear Kalman filer was applied to the linearized model to estimate the state vector of the linearized system. Unlike an extended Kalman filter (EKF), the DKF provides state estimation without using derivatives or Jacobians. The result is the avoidance of drawbacks of the EKF concerning local linearization using first-order Taylor series expansion. This is an important advantage because these problems can affect the accuracy of state estimation, and consequently the stability and performance of the state estimation-based controller.

1.3 Outline of Thesis

Chapter II provides an introduction to nonlinear control systems. It highlights the importance of nonlinear control design and introduces various types of system nonlinearity. Two significant nonlinear control design objectives (stabilization and trajectory tracking) are discussed. Additionally, common nonlinear control methods are introduced. In the last part of the chapter, feedback linearization is introduced as a powerful nonlinear control technique. The chapter concludes with a discussion of input state linearization and the standard linear Kalman filter for estimation-based control design, along with an illustrative example of DC-servo position control.

Chapter III reviews input-output linearization for a class of nonlinear systems, which are illustrated with a robotic system. To achieve estimation-based control, a standard Kalman filter is applied to the linearized model for state estimation. This approach is known as derivative-free Kalman filtering (DKF). The remainder of the chapter comprises some of the original contributions of this thesis. First, a three-DOF robot / prosthesis system that is disturbed by ground reaction force (GRF) is introduced as an illustrative example of an MIMO system. Next, PI and PD supervisory control terms are introduced to make the closed-loop system robust to the unknown GRF.

Chapter IV begins by reviewing stability for nonlinear systems. It provides a short introduction to the concepts, definitions, and types of stability. Next, the chapter reviews Lyapunov stability theorems and invariant set theorems. Next, the chapter provides stability analyses of linear systems via Lyapunov candidate functions, along with stability analyses of non-autonomous systems. The rest of the chapter concludes the original contribution of this thesis by providing a stability analysis of the DKF from Chapter III in the frequency domain, along with an error convergence analysis.

Chapter V concludes the thesis and provides suggestions for future research.

CHAPTER II

NONLINEAR CONTROL DESIGN

In this chapter we start with a short introduction to nonlinear control systems to highlight the importance of nonlinear control and to introduce different types of nonlinearity. Two major control design objectives are discussed (stabilization and trajectory tracking). Additionally, common nonlinear control methods are introduced. Finally, we present feedback linearization, input-state linearization, and the standard Kalman filter for estimation-based control, along with an illustrative SISO example of DC-servo position control.

2.1 The Importance of Nonlinear Control

The importance of nonlinear control is based on the fact that all physical systems are inherently nonlinear, and so we need to consider these nonlinearities in our control designs [59, Chapter 1]. For instance, consider the control of a robot manipulator using a simple linear PID controller with gravity compensation. In a small range of operation, the controller can provide a satisfactory response. However, when motion at high speed is needed, the controller's performance can dramatically decrease. This may be the result of the robot's nonlinearity. Coriolis and centripetal forces are two basic nonlinearities that increase with the square of the speed in electromechanical systems like electric motors.

The requirement for operation over large ranges of system parameter values, fast

response, and high accuracy, especially in trajectory tracking, has motivated the development of nonlinear control. Although nonlinear control in many cases can provide a better solution than linear control, it has natural shortcomings that can affect the control design. Multiple equilibrium points, limit cycles, bifurcations due to parameter changes, and chaos (extremely high dependence of the output on the initial conditions) are some examples of undesired behavior [59, Chapter 1].

2.1.1 Model and Parameter Uncertainties

Again, consider a robot manipulator. Suppose the robot task is to pick an object from one place and put it in another location. In linear control design we are generally not concerned with initial conditions and the system parameters are generally considered to be well known. Changes in (for example) mass are not considered by the controller, potentially causing poor performance or instability. (Note that if the controller adapts to changes in mass, then the controller has become nonlinear.) Parameter changes can cause problems in linear systems given the general assumption of a well-defined model with no uncertainty, and the independence of the control system on parameter changes.

Now consider a nonlinear controller that is designed to perform the same task but that considers the mass as a parameter that can be compensated. A good example of this type of nonlinear controller is an adaptive controller. The adaptation law makes the control design, as a whole, nonlinear. This provides the potential for a better, smoother, more stable, and more accurate response. In some systems, like aircraft or process control, parameter changes occur slowly. However, in other systems such as robotics, parameter changes can occur quickly [59, Chapter 1].

2.1.2 Hard Nonlinearities

Hysteresis, dead zones, saturation, backlash, and Coulomb friction are known as hard nonlinearities. This is due to their discontinuous nature, which does not allow approxima-

tion via linearization. Since linear control techniques require linearization, these types of nonlinearities are neglected by linear controllers. One of the advantages of nonlinear controllers is that they can potentially handle these types of nonlinearities through prediction and compensation.

2.2 Nonlinear System Definitions and Discussion

2.2.1 Design Objectives for Nonlinear Systems

For most control system designs:

1. A given physical nonlinear system is required to be controlled.
2. The desired behavior of the controlled system is specified.
3. A closed-loop feedback controller is designed to achieve the desired behavior and achieve stability of the closed-loop system.

We face two primary challenges in controller design. The first challenge is stabilization around an equilibrium point. Consider a nonlinear system with dynamics

$$\dot{x} = f(x,u,t) \tag{2.1}$$

where x is the state, u is the control, and t is time. The objective is to find a control input u such that starting at any point in a defined state-space region $\mho$ (called the region of attraction), $x \to 0$ as $t \to \infty$. For instance, assume we have a nonlinear system described as

$$k_1\ddot{x} - k_2 \sin(\pi x) = u \qquad \text{with} \quad k_1, k_1 > 0 \tag{2.2}$$

The control input u can be designed as a PD term to provide state feedback and a feedforward term to cancel the system nonlinearity:

$$u = -k_d\dot{x} - k_p x - k_2 \sin(\pi x) \tag{2.3}$$

where k_d and k_p are positive user-specified tuning parameters. This control input results in a globally stable closed-loop system:

$$k_1\ddot{x} + k_d\dot{x} + k_p x = 0 \tag{2.4}$$

The second challenge in controller design is to track a reference trajectory. Consider a nonlinear system

$$\dot{x} = f(x,u,t)$$

$$y = h(x) \tag{2.5}$$

with desired trajectory $y = y_d$. The objective is to design a control input u such that starting at any point in state space region $\mho$, $y - y_d \to 0$, while all states x remain bounded [59, Chapter 3]. An example of this type of control problem will be discussed at the end of this chapter.

2.2.2 Feedback and Feedforward in Nonlinear Control Design

Feedback is a crucial factor in all systems (both linear and nonlinear) for stabilizing closed-loop systems. The design of feedback gains can be achieved using pole placement for linear systems.

Feedforward in control design cancels known disturbances, uncertainties, or nonlinearities that are associated with the system dynamics. It is difficult to attain trajectory

tracking without canceling nonlinearities through feedforward.

$$u_{\text{total}} = u_{\text{feedback}} + u_{\text{feedforward}}$$

2.3 Common Nonlinear Control Design Methods

Unlike linear systems, the design of control methods for nonlinear systems is system-specific, and so there are no universal methods for nonlinear control design. However, depending on the system's properties, we can identify certain classes of nonlinear systems and discuss common control techniques [59, Chapter 5].

2.3.1 Trial and Error

As the name suggests, this general approach to solving control problems can be useful, though only in simple cases. In this method, knowledge of the system dynamics is useful, when combined with experience and intuition [59, Chapter 5].

2.3.2 Feedback Linearization

The idea of this technique is that some classes of nonlinear systems can be transformed to new state-space coordinates. These new coordinates are simpler than the original coordinates, which in turn facilitates the design of a nonlinear controller and the subsequent stability analysis. This linearization technique can be used either partially or fully, depending on the system dynamics.

Feedback linearization can be applied only to certain classes of nonlinear systems, and so it cannot be viewed as a universally applicable technique. Input-state and input-output linearization are two common variations of this method. This method is a powerful control method, and it provides the structure for other nonlinear control techniques [59, Chapter 6]. One of the main drawbacks of this technique is that it is not robust

to model uncertainty. This control methodology will be discussed in detail later in this thesis.

2.3.3 Robust Control

Exact feedback linearization relies on the assumption that the system can be accurately modeled. Uncertainties in parameters and in the system model cannot be handled well be feedback linearization. Robust control can provide a solution to this problem by using knowledge about the uncertainties. For instance, information about the bounds of parameter variations can be used. In other words, exact feedback linearization is not capable of compensating for uncertainties, which results in the requirement for an additional control term that can be provided by robust control, which can in turn stabilize the system [59, Chapter 7].

$$u_{\text{total}} = u_{\text{feedback-linearization}} + u_{\text{robust}}$$

2.3.4 Adaptive Control

Adaptive control is another method that can be combined with feedback linearization. Adaptive control compensates for gradual parameter changes in well-defined dynamic models. This technique can complement robust control, or can serve as an alternative to robust control. Adaptive control is usually applied to time-varying or uncertain systems [59, Chapter 8].

$$u_{\text{total}} = u_{\text{feedback-linearization}} + u_{\text{robust}} + u_{\text{adaptive}}$$

2.4 Feedback Linearization

In this section, feedback linearization is discussed in detail. As an illustration, a DC motor with nonlinear dynamics is controlled with input-state linearization and a linear estimator

(Kalman filter).

Feedback linearization is a powerful control method for nonlinear systems. The key feature of feedback linearization is the transformation of a nonlinear system from its original state-space coordinates to a new coordinate system, resulting in a system that is fully or partially linear. Canceling nonlinearities in a nonlinear system results in a linear system such that highly efficient linear control methods (for example, Hurwitz pole placement) can be easily applied.

Feedback linearization has been used to address practical control problems such as the control of helicopters, high performance aircraft, industrial robots, biomedical devices, and industrial applications. However, there are also a number of notable shortcomings and limitations associated with this approach, which are topics of current research [59, Chapter 6]. One issue that arises is the question of what class of nonlinear system is suitable for feedback linearization. Feedback linearization can be applied to nonlinear systems that are in controllable canonical form, or companion form [59, Chapter 6], among other systems (as will be clarified later in this section).

Definition 2.4.1 *If the dynamics of a system can be written in the form*

$$x^n = f(x) + g(x)u \tag{2.6}$$

then the system is said to be in controllable canonical form, or companion form.

In the above equation, u is the control input, x is the the state vector, and $f(x)$ and $b(x)$ are nonlinear functions. Eliminating the nonlinearity with the control

$$u = \frac{v - f}{g} \tag{2.7}$$

where $g \neq 0$ in the scalar case, and g is an invertible matrix in the multidimensional case,

results in the closed-loop linear system

$$x^n = v$$

where v is called the virtual control, which can be designed to achieve closed-loop stability, meaning that the roots of the closed-loop transfer function are strictly negative.

$$v = -k_0 x - k_1 \dot{x} - \ldots - k_{n-1} x^{(n-1)} \quad \text{where } k_i > 0 \tag{2.8}$$

$$x^{(n)} + k_{n-1} x^{(n-1)} + \ldots + k_0 x = 0$$

The virtual control can also be designed to achieve exponentially stable error dynamics for trajectory tracking:

$$\begin{aligned} v &= -k_0 e - k_1 \dot{e} - \ldots - k_{n-1} e^{(n-1)} + x_d^{(n)} \quad \text{where } k_i > 0 \\ e &= x - x_d \\ 0 &= e^{(n)} + k_{n-1} e^{(n-1)} + \ldots + k_0 e \end{aligned} \tag{2.9}$$

where x_d is the desired state trajectory.

As mentioned earlier, feedback linearization can be implemented in two ways, under certain conditions. Implementing these methods requires the use of differential geometry and other advanced mathematics [59, Chapter 6]. Some definitions and relationships are introduced next to provide background and to provide a foundation for the later examples.

Input-State Linearization

Consider the following SISO nonlinear system (the MIMO case will be discussed later):

$$\dot{x} = f(x, u) \tag{2.10}$$

Input state linearization can then be applied in two steps [59, Chapter 6].

1. A state transformation $z = z(x)$ and an input transformation $u = u(x, v)$ are found such that the nonlinear system dynamics are transformed into the equivalent linear time-invariant dynamics, $\dot{z} = Az + bv$, where v is the virtual control term.

2. A linear control design method like Hurwitz pole placement is used to design the virtual control term.

The following definitions are provided as background to a theorem that will be presented later in this section to state the conditions for the existence of the input-state linearization of a nonlinear system. In all definitions and theorems in this thesis, the term smooth indicates a function that is differentiable up to any order.

1. A vector function $f : R^n \to R^n$ is called a vector field in R^n.

2. Given a smooth scalar function $h(x)$, the gradient of $h(x)$ is denoted by the n-element vector ∇h:

$$\nabla h = \frac{\partial h}{\partial x} \tag{2.11}$$

3. Given a smooth vector field $f(x)$, the Jacobian of $f(x)$ is denoted by the $n \times n$ matrix

$$\nabla f = \frac{\partial f}{\partial x} \tag{2.12}$$

4. Let $h : R^n \to R$ be a smooth scalar function, and $f : R^n \to R^n$ be a smooth vector field on R^n. Then the Lie derivative of h with respect to f is a scalar function defined by the dot product

$$L_f h = \underbrace{\nabla h}_{Gradient} \cdot f \tag{2.13}$$

5. Let f and g be two vector fields on R^n. The Lie bracket of f and g is a vector field

defined by

$$[f,g] = \underbrace{\nabla g}_{Jacobian} \cdot f - \underbrace{\nabla f}_{Jacobian} \cdot g \tag{2.14}$$

The Lie bracket $[f,g]$ is commonly written as $ad_f g$.

6. A function $\psi : R^n \to R^n$, defined in a region $\mho$, is called a diffeomorphism if it is smooth and if its inverse ψ^{-1} exists and is smooth.

7. Let ψ be a smooth function defined in a region $\mho$ in R^n. If the Jacobian matrix $\nabla\psi$ is non-singular at a point $x = x_0$ in $\mho$, then $\psi(x)$ defines a local diffeomorphism in a subregion of $\mho$. Note that a diffeomorphism is a one-to-one transformation to a new coordinate system, so if there are no singular points associated with the transformation, then the inverse exists; that is, $x = \psi^{-1}(z)$.

8. If the Lie bracket of f and g can be expressed as a linear combination of f and g, it satisfes a condition called the involutivity condition between f and g.

9. A set of vector fields $[f,g]$ is completely integrable if and only if it is involutive.

10. If a given nonlinear system is in the form (2.6) in which $f(x)$ and $g(x)$ are smooth vector fields in R^n, then there exists a diffeomorphism $\psi : \mho \to R^n$ in a state-space region $\mho$ in R^n with

$$u = \alpha(x) + \beta(x)v \tag{2.15}$$

such that the virtual control input v and the new state variable $z = \psi(x)$. The transformed system is linear.

Given the above definitions, the following theorem can now be stated [59, Chapter 6].

Theorem II.1 *A nonlinear system in the form (2.6) in which $f(x)$ and $g(x)$ are both smooth vector fields in R^n is input-state linearizable if and only if there exists a state-space region $\mho$ such that the the following conditions hold.*

1. The set $\{g, ad_f g, ..., ad_{f^{n-1}} g\}$ is linearly independent in the region $\mho$ (controllability).

2. The set $\{g, ad_f g, ..., ad_{f^{n-2}} g\}$ is involutive in the region $\mho$.

Input-state linearization can be achieved with the following procedure.

1. Construct the vectors $g, ad_f g, ..., ad_{f^{n-1}} g$.

2. Verify the controllability and involutivity conditions.

3. Select the first transformed state $z_1 = \psi(x)$ such that the following equalities are satisfied:

$$\underbrace{\nabla z_1}_{Gradient} \cdot ad_{f^i} g = 0 \qquad i = 0, 1, ..., n-2 \tag{2.16}$$

$$\underbrace{\nabla z_1}_{Gradient} \cdot ad_{f^{n-1}} g \neq 0 \tag{2.17}$$

4. Compute the state transformation and input transformation:

$$z(x) = [z_1, L_f z_1, ..., L_{f^{n-1}} z_1] \tag{2.18}$$

$$\alpha(x) = \frac{L_f^n z_1}{L_g L_f^n z_1} \tag{2.19}$$

$$\beta(x) = \frac{1}{L_g L_f^{n-1} z_1} \tag{2.20}$$

Estimation-Based Feedback Linearization

State and parameter estimation of nonlinear systems has received much attention from scholars and industry and remains an interesting and current research area. This attention is due to the fact that state estimation provides the opportunity for sensorless, efficient control. Additionally, an optimal observer makes it possible to use a relatively accurate control feedback signal, resulting in improved controller performance. One of the many areas of estimation-based control is electromechanical energy conversion. Sensorless control of motors and generators has been a research interest for many decades, resulting in

many commercialized estimation-based motor control approaches. Permanent magnet synchronous motors (PMSMs), brushless DC motors (BLDCs), permanent magnet DC motors (PMDCs), and induction motors (IMs) are electromechanical actuators that can be controlled with these estimation-based approaches, and focus on speed, current, back-emf, and rotor resistance estimation.

Since feedback linearization relies on full state information, an observer can provide an opportunity to obtain the full state without having a hardware sensor. This feature can add flexibility to the control of systems in case of the loss of one or more measurements, enabling the system to maintain desired performance.

Example: Nonlinear Electromechanical System

This example is based on [52]. Figure 1 shows a DC motor schematic that includes an electric circuit and a mechanical model.

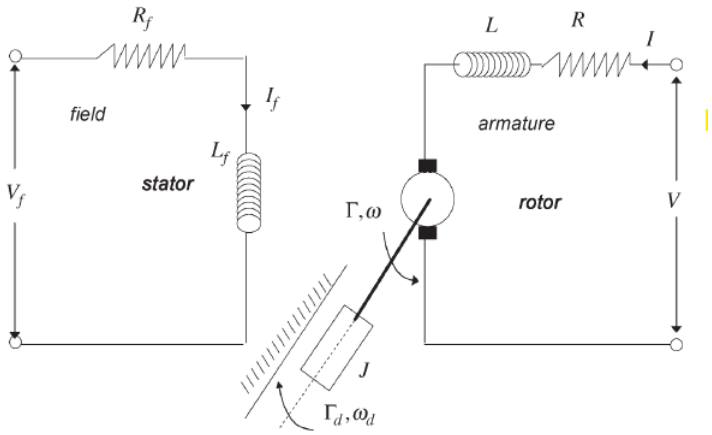

Figure 1: DC Motor Schematic

DC motors have linear dynamics but can exhibit nonlinear behavior in the presence of state-dependent external torque. In practice, a DC motor is nonlinear due to armature reaction effects, which can be somewhat mitigated by adding a small compensator

pole (winding) to the stator. The DC motor dynamics are given as

$$L\frac{dI}{dt} = -K_e\omega - RI + V \tag{2.21}$$

$$J\dot{\omega} = K_e I - K_d\omega - \Gamma_d \tag{2.22}$$

where L denotes armature inductance, I denotes armature current, K_e denotes the motor's electrical constant, R denotes armature resistance, V denotes input voltage, J denotes motor inertia, ω denotes rotor rotation speed, K_d denotes the mechanical damping constant, and Γ_d denotes the disturbance or external torque. We suppose here that $\Gamma_d = mgl\sin\theta$, which creates a nonlinearity in the DC motor dynamics. Suppose that the DC motor rotates a rigid link of length l with a mass m attached to its end. The state vector is $[x_1, x_2, x_3]^T = [\theta, \dot{\theta}, \ddot{\theta}]^T$, where θ is the rotation angle of the motor, which is considered the system output $y(t)$. The nonlinear model of the DC motor is then given in affine form as

$$\dot{x} = f(x,t) + g(x,t)u$$

where both f and g are vector fields:

$$f = \begin{bmatrix} f_1 \\ f_2 \\ f_3 \end{bmatrix} = \begin{bmatrix} x_2 \\ x_3 \\ -(K_e^2 + \frac{K_d R}{JL})x_2 - (RJ + \frac{K_d L}{JL})x_3 - (\frac{Rmgl}{JL})\sin x_1 - (\frac{mgl}{J})x_2\cos x_1 \end{bmatrix} \tag{2.23}$$

$$g = \begin{bmatrix} 0 \\ 0 \\ -\frac{K_e}{JL} \end{bmatrix} \tag{2.24}$$

The nonlinear dynamics of the motor can be written as

$$x^{(n)} = f_n(x) + g_n(x)u \qquad \text{where } n = 3 \tag{2.25}$$

The following form is an equivalent equation in linear observer canonical form that is appropriate for the application of the standard Kalman filter.

$$\begin{aligned} \dot{x}_1 &= x_2 \\ \dot{x}_2 &= x_3 \\ \dot{x}_3 &= v \end{aligned} \tag{2.26}$$

where v is the virtual control signal. Figure 2 shows the schematic of the DC motor in an estimation-based control configuration. There is a block for the nonlinear estimator and a block for the nonlinear controller. Inside the nonlinear estimator block, the combination of the linearization transformation and the linear Kalman filter is a nonlinear block. The virtual control term, which is constructed as a nonlinear function of the physical control signal, is input to the Kalman filter. In this example the control objective is trajectory tracking, meaning the motor angle θ should follow a desired trajectory θ_d.

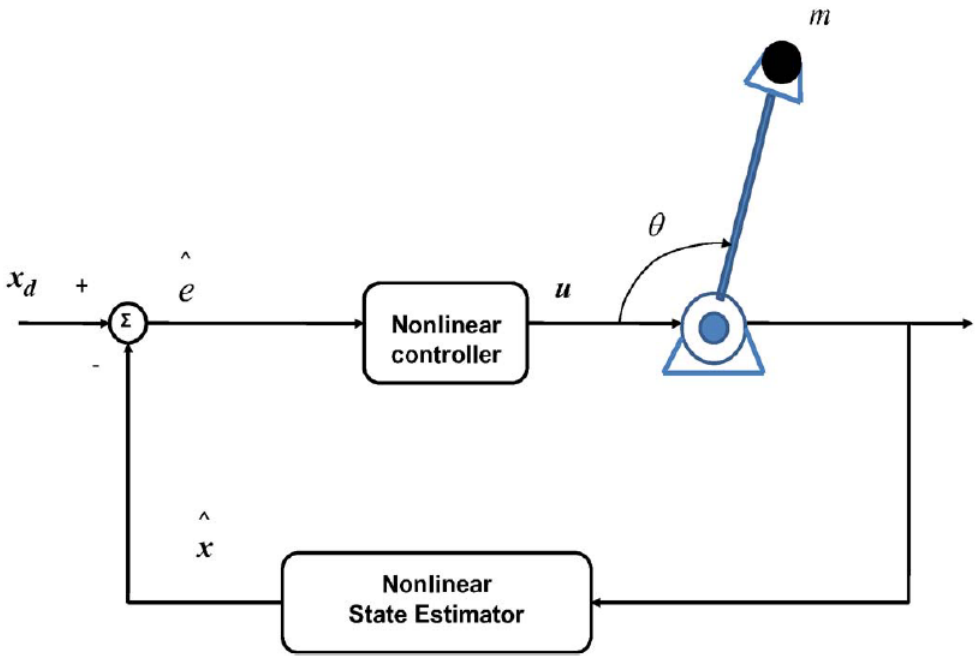

Figure 2: Closed-loop estimation-based control of a DC motor

The error term is defined as $e = x_d - \hat{x}$, and the control voltage is computed as

$$u = \frac{1}{g_n(\hat{x})}[x_d^{(n)} - f_n(\hat{x}) - K^T e], \qquad n = 3, \quad K > 0 \tag{2.27}$$

The final form of the system as transformed from its original nonlinear form to a linear form is given as

$$\begin{aligned} \dot{Z}(t) &= AZ(t) + Bv(t) + M\gamma(t) \\ y(t) &= CZ(t) + \varpi(t) \end{aligned} \tag{2.28}$$

where A, B, C, and M are the system matrix, the control input matrix, the measurement matrix, and the noise input matrix. $\gamma(t)$ and $\varpi(t)$ represent the process and measurement noise terms. The Kalman filter for this linear system is given as

$$\begin{aligned} \hat{Z}(0) &= E[Z(0)] \\ P(0) &= E\left[\left(Z(0) - \hat{Z}(0)\right)\left(Z(0) - \hat{Z}(0)\right)^T\right] \\ K(t) &= P(t)C^T R^{-1}(t) \\ \dot{\hat{Z}}(t) &= A\hat{Z}(t) + Bv(t) + K(t)(y(t) - C\hat{Z}(t)) \\ \dot{P}(t) &= AP(t) + P(t)A^T(t) + Q(t) - P(t)C^T R^{-1}(t)CP(t) \end{aligned} \tag{2.29}$$

where $K(t)$ and $P(t)$ are the Kalman gain matrix and the estimation error covariance matrix. The covariance of the process noise and the measurement noise are $Q(t) = E\left[\gamma(t)\gamma^T(t)\right]$, and $R(t) = E\left[\varpi(t)\varpi^T(t)\right]$, respectively.

Simulation Results

Here we present trajectory tracking with a sinusoidal reference signal. Hurwitz pole placement can be used to obtain the feedback gains $K = [100,\ 80,\ 60]^T$, where K_1 is the coeffi-

cient corresponding to $\ddot{e}$, K_2 is the coefficient corresponding to $\dot{e}$, and K_3 is the coefficient corresponding to e, which results in a closed-loop transfer function denominator polynomial with poles that have strictly negative real parts:

$$s^3 + 100s^2 + 80s + 60 = 0 \rightarrow s_1 = -58.66,\ s_2 = -0.66 + 1.12i,\ s_3 = -0.66 - 1.12i$$

Figures 3, 4, and 5 compare the simulated values of motor angle, velocity, and acceleration with their reference values, and shows good tracking performance in spite of initial condition errors. Figures 6, 7, and 8 compare the actual values of motor angle, velocity, and acceleration with their estimated values, showing good estimation in spite of initial condition errors. Figure 9 compares the actual control signal and the virtual control signal.

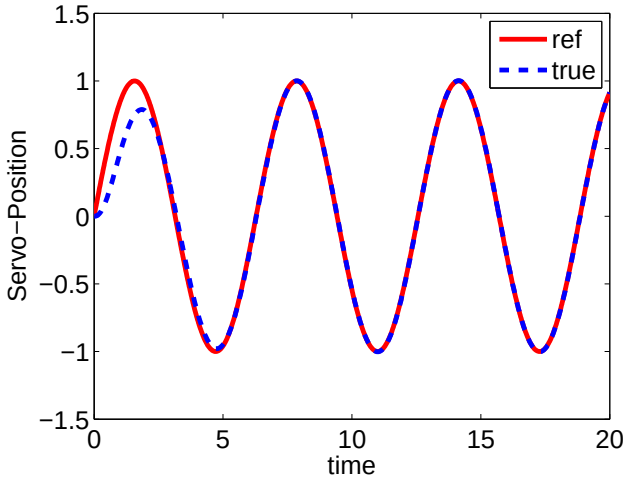

Figure 3: Simulated DC motor angle compared with desired trajectory

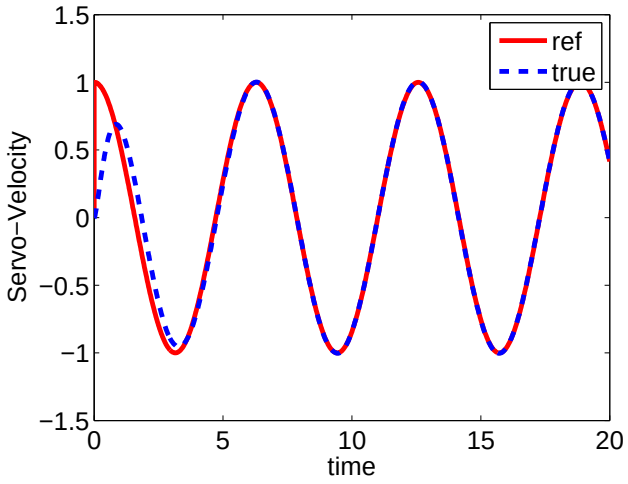

Figure 4: Simulated DC motor velocity compared with desired trajectory

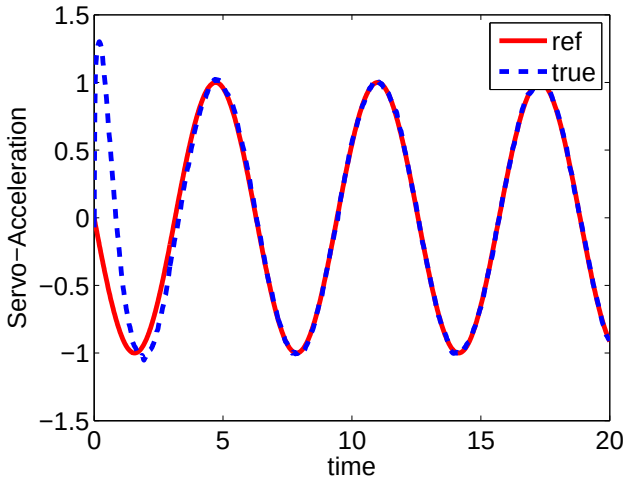

Figure 5: Simulated DC motor acceleration compared with desired trajectory

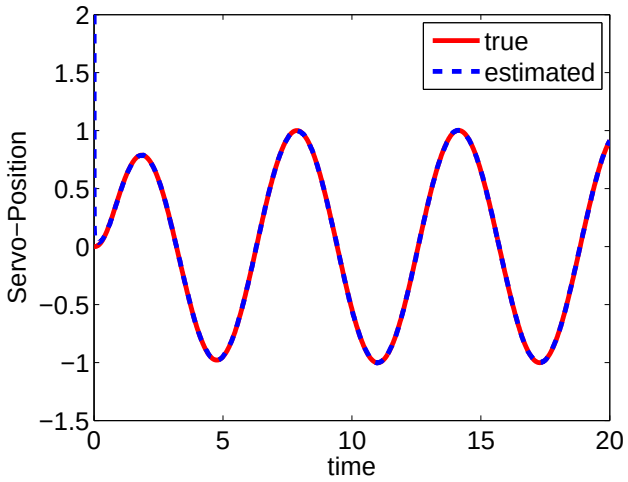

Figure 6: Simulated DC motor angle compared with estimated value

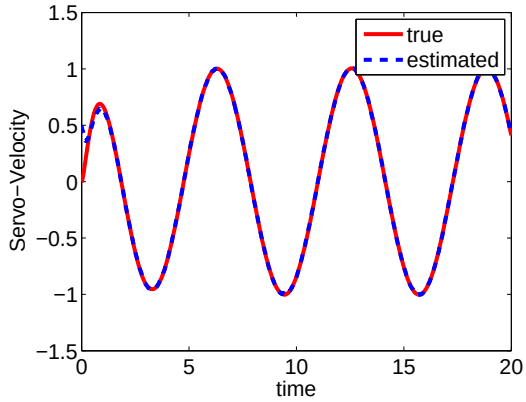

Figure 7: Simulated DC motor velocity compared with estimated value

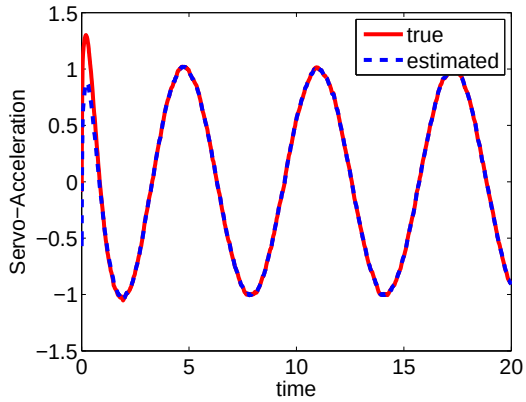

Figure 8: Simulated DC motor acceleration compared with estimated value

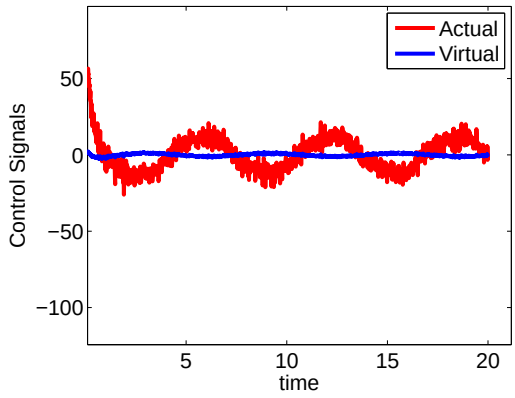

Figure 9: DC motor example: actual and virtual control signals

2.5 Discussion

This chapter provided an introduction to nonlinear control. It highlighted the importance of nonlinear control and introduced different types of system nonlinearity. Two main nonlinear control design objectives (stabilization and trajectory tracking) were discussed. Some common nonlinear control methods were briefly introduced. Finally, feedback linearization and system transformation were introduced. Input-state linearization and standard Kalman filtering, which comprise estimation-based control, was presented, along with an illustrative SISO example of DC-servo position control. The simulation results showed that a linearized system, along with a linear observer (Kalman filter), is capable of handling a large initial error, which is notable in comparison with nonlinear observers like the EKF and the UKF.

Feedback linearization can provide a desirable solution for certain classes of nonlinear systems. This method can be applied in two ways: input-state linearization, and input-output linearization. In practice, input-state linearization is a special case of input-output linearization, which will be discussed in the next chapter.

CHAPTER III

DERIVATIVE-FREE KALMAN FILTER-BASED CONTROL OF PROSTHETIC LEGS

Derivative-free Kalman filter-based control for a special class of nonlinear systems was introduced in [52] and showed improved performance of estimation and tracking compared to other nonlinear filter / control methods. Much of the content of this chapter is based on [43].

We develop a derivative-free Kalman filter (DKF) for state estimation-based control for a general n-DOF robotic system. We then propose a robust DKF when the robot dynamics are affected by disturbances / unknown inputs. In the robust DKF, we use two different methods for disturbance rejection: PD and PI disturbance compensators. These methods provide supervisory control, making the DKF more robust in the presence of disturbances / unknown inputs.

The system considered here is a combination of a test robot that emulates human hip and thigh motion, and a powered transfemoral prosthetic leg. The robot / prosthesis combination is modeled as a robot with three degrees of freedom (DOFs): vertical hip displacement, thigh angle, and knee angle. Simulation results show the advantages of

applying the DKF and the robust DKF to the three-DOF robot / prosthesis system for state estimation-based control.

3.1 Derivative-Free Kalman Filtering for Robotic Systems

The Kalman filter applies directly only to linear systems. However, we can linearize a nonlinear system for control purposes and then use linear estimation techniques. Applying the standard Kalman filter to a nonlinear system through the transformation of the original nonlinear system to observer canonical form is called derivative-free Kalman filtering (DKF). The linearization transformation of the nonlinear system is based on a diffeomorphism and does not involve the computation of Jacobians. The DKF can be used for estimation-based control of robots if the system model is subjected to exact feedback linearization control, followed by state estimation of the linearized model with the standard Kalman filter.

A dynamic model of a multi-input-multi-output (MIMO) n-DOF robot is given as

$$M(q)\ddot{q} + C(q,\dot{q})\dot{q} + J_e^T F_e + G(q) = u \tag{3.1}$$

where q is the vector of generalized joint angles, $M(q)$ is the mass matrix, $C(q,\dot{q})$ is a matrix accounting for centripetal and Coriolis effects, J_e is the kinematic Jacobian relative to the point of application of the external forces F_e, $G(q)$ is the gravity vector, and u is the vector of control signals [6, 19, 50, 51]. The details of these matrices and the system parameters of the robot / prosthesis system are given in Appendix A. We first assume that the system model (3.1) is known in its model parameters and inputs and there are no unknown inputs to the system except random noise terms. The robot's dynamic model (3.1) can be written in affine state space form with the inclusion of noise terms in the process

and measurement equations as

$$\begin{aligned} \dot{x} &= f(x,t) + g(x,t)u + \omega(t) \\ y &= h(x,t) + \varpi(t) \end{aligned} \tag{3.2}$$

where the state vector $x(t)$, the input $u(t)$, and the output $y(t)$ are in $\mathbb{R}^n$, $\mathbb{R}^p$ and $\mathbb{R}^m$ respectively; and the smooth vector fields $f(.)$ and $g(.)$ are in $\mathbb{R}^n$ and $\mathbb{R}^{n\times p}$ respectively. The noise terms $\omega(t)$ and $\varpi(t)$ are bandlimited, zero-mean, and uncorrelated. The process noise is partially due to parameter uncertainty, partially due to input certainity, and partially due to unmodeled dynamics. The measurement noise corresponds to errors in the measurement equipment. The nonlinear system (3.2) is subjected to a linearization transformation to obtain an observer canonical form in order to perform derivative-free Kalman filtering (DKF) [52]. Since the linearization transformation of MIMO systems requires an invertible decoupling matrix, we assume that the number of inputs is equal to the number of outputs; $p = m$. The dynamic model is input-output linearizable under the conditions given in [59, Chapter 6]. Therefore, classic input-output linearization can be applied by differentiating the output functions y_i $(i = 1,2,..,m)$ until the inputs appear.

We assume that the flat output of the system [53, Chapter 2] is a linear function of the state vector elements. In this case, the applied transformation does not have any nonlinear effects on the noise signals. We also assume that we know the mean and covariance of the noise so that we can calculate the mean and covariance of the differentiated noise [49, Chapter 9].

Assume that r_i is the smallest integer such that at least one of the inputs appears in $y_i^{(r_i)}$. Then

$$y_i^{(r_i)}(t) = L_f^{r_i} h_i(x) \sum_{j=1}^{m} L_{g_j} L_f^{r_i-1} h_i(x) u_j(t) + \gamma_i(t) \tag{3.3}$$

where $L_f h$ denotes for the Lie derivative $L_f h = (\nabla h) f$, with $L_{g_j} L_f^{r_i-1} h_i \neq 0$; and $\gamma_i(t)$ is

noise with zero mean:

$$\gamma_i(t) = \omega_i(t) + \frac{\mathrm{d}}{\mathrm{dt}}^{r_i} \varpi_i(t) \tag{3.4}$$

Note that one of the benefits of transforming the robot dynamics (3.1) into affine state-space form (3.2) is to handle the noise terms of the diffeomorphism. Based on (3.3) and exact feedback linearization, the system model (3.2) (ignoring noise) can be transformed into the following form [59, Chapter 6]:

$$\begin{bmatrix} v_1(t) \\ \vdots \\ v_m(t) \end{bmatrix} = \begin{bmatrix} L_f^{r_1} h_1(x) \\ \vdots \\ L_f^{r_m} h_m(x) \end{bmatrix} + \Gamma(x)u(t) \tag{3.5}$$

where $\Gamma(x)$ is the $m \times m$ invertible decoupling matrix, and the scalar $r = r_1 + r_2 + \ldots + r_m$ is called the total relative degree of the system. The virtual control terms $v_i(t)$ will be designed later in this chapter. When the partial relative degrees r_i are integers such that $L_{g_j} L_f^{r_i - 1} h_i \neq 0$, then the input transformation

$$u(t) = \Gamma^{-1}(x) \begin{bmatrix} v_1(t) - L_f^{r_1} h_1(x) \\ \vdots \\ v_m(t) - L_f^{r_m} h_m(x) \end{bmatrix} \tag{3.6}$$

yields m linear systems, which include the noise terms $\gamma_i(t)$ from (3.3):

$$\begin{aligned} \dot{Z}_1^i(t) &= Z_2^i(t) \\ &\vdots \\ \dot{Z}_{r_i}^i(t) &= y_i^{(r_i)}(t) = v_i(t) + \gamma_i(t), \qquad i = 1, 2, \ldots, m \end{aligned} \tag{3.7}$$

Now we can write an individual state space equation for every decoupled subsystem:

$$\dot{Z}^i(t) = A_i Z^i(t) + B_i v_i(t) + M_i \gamma_i(t)$$
$$y_i(t) = C_i Z^i(t) + \varpi_i(t) \tag{3.8}$$

Equation (3.8) is written in state space canonical form as

$$\begin{bmatrix} \dot{Z}_1^i(t) \\ \dot{Z}_2^i(t) \\ \vdots \\ \dot{Z}_{r_i}^i(t) \end{bmatrix} = \overbrace{\begin{bmatrix} 0 & 1 & \cdots & 0 \\ \vdots & 0 & \ddots & 0 \\ 0 & \cdots & 0 & 1 \\ 0 & \cdots & \cdots & 0 \end{bmatrix}}^{A_i} \begin{bmatrix} Z_1^i(t) \\ Z_2^i(t) \\ \vdots \\ Z_{r_i}^i(t) \end{bmatrix} + \overbrace{\begin{bmatrix} 0 \\ 0 \\ \vdots \\ 1 \end{bmatrix}}^{B_i} v_i(t) + \overbrace{\begin{bmatrix} 0 \\ 0 \\ \vdots \\ 1 \end{bmatrix}}^{M_i} \gamma_i(t)$$
$$y_i(t) = \underbrace{\begin{bmatrix} 1 & 0 & \cdots & 0 \end{bmatrix}}_{C_i} Z_i(t) + \varpi_i(t) \tag{3.9}$$

for $i = 1, ..., m$. After input-output linearization and the derivation of the transformed models for each subsystem, linear control laws (virtual controls) v_i can be obtained to control each transformed subsystem (3.9). The controller is designed to make the system output follow a desired trajectory Z_d. The virtual control is defined for each subsystem as

$$v_i(t) = Z_{di}^{(r_i)}(t) - \theta_i^T e_i(t) \tag{3.10}$$

where the gain matrix $\theta_i^T = \left[\theta_{r_i}^i, \ldots, \theta_1^i\right]^t$ is designed by pole placement and the error dynamics is obtained from the estimation errors $e_i(t) = \hat{Z}_i - Z_{di}$ with $e_i(t) = \left[e_i, \dot{e}_i, \ldots, e_i^{(r_i-1)}\right]^T$ such that the polynomial $e_i^{(r_i)} + \theta_1^i e_i^{r_i-1} + \ldots + \theta_{ri}^i e_i$ is Hurwitz. To obtain the estimate of the state vector $\hat{Z}_i$, we apply the standard Kalman filter to the linearized model of the robot

(3.9) as follows [58, Chapter 8].

$$
\begin{aligned}
\hat{Z}_i(0) &= E[Z_i(0)] \\
P_i(0) &= E\left[\left(Z_i(0)-\hat{Z}_i(0)\right)\left(Z_i(0)-\hat{Z}_i(0)\right)^T\right] \\
K_i(t) &= P_i(t)C_i^T R_i^{-1}(t) \\
\dot{\hat{Z}}_i(t) &= A_i\hat{Z}_i(t)+B_i v_i(t)+K_i(t)(y_i(t)-C_i\hat{Z}_i(t)) \\
\dot{P}_i(t) &= A_iP_i(t)+P_i(t)A_i^T(t)+Q_i(t)-P_i(t)C_i^T R_i^{-1}(t)C_iP_i(t)
\end{aligned} \tag{3.11}
$$

for $i = 1,...,m$, where $K_i(t)$ and $P_i(t)$ are the Kalman gain and estimation error covariance matrix, and the covariances of the process and measurement noise are $Q_i(t) = E\left[\gamma_i(t)\gamma_i^T(t)\right]$ and $R_i(t) = E\left[\varpi_i(t)\varpi_i^T(t)\right]$, respectively. We see that a Kalman filter can be designed for each decoupled subsystem, $i = 1,\ldots,m$, separately. These two steps, feedback linearization and decoupled state estimation by standard Kalman filters, comprise the DKF. The Kalman filter provides estimates of the states for input to the feedback linearization controller.

3.2 Derivative-Free Kalman Filtering in the Presence of Unknown Inputs

Parameter uncertainties and external disturbances are unknown inputs that can affect the robot model. In robotic systems, unknown inputs can result from the following [53]: (i) uncertainties and changes in the model parameters, (ii) unknown external torques exerted on the robot joints, (iii) unknown external forces exerted on the masses of the robotic mechanism. In the DKF we use feedback linearization to linearize the nonlinear model of the robot so that we can apply the standard Kalman filter. However, the performance of the DKF may suffer since feedback linearization is not robust in the presence of disturbances and unknown inputs. In this section, the DKF for state estimation-based control is considered in the presence of unknown inputs.

The robot's dynamic model in (3.2) can be written in affine state space with unknown inputs as

$$\dot{x} = f(x,t) + g(x,t)u + \varpi(t) + E(x,t)\,d(x,t)$$

$$y = h(x,t) + \varpi(t) \tag{3.12}$$

where $d(x,t) \in \mathbb{R}^l$ is the unknown input vector and $E(x,t)\,d(x,t)$ comprises the effect of the unknown inputs on each joint, where $E(x,t) \in \mathbb{R}^{n\times l}$ can be calculated from the dynamic model (3.1). The unknown input and its derivatives are assumed to be bounded, but the bounds are unknown and we do not have any information about the dynamics of the unknown inputs. The approach of Section 3.1 is used here for the linearization of the model (3.12). Exact feedback linearization is applied and the input transformation is obtained from (3.6), which results in the transformation of (3.12) into the m decoupled subsystems

$$\begin{aligned}
\dot{Z}_1^i(t) &= Z_2^i(t) \\
&\vdots \\
\dot{Z}_{r_i}^i(t) &= y_i^{(r_i)}(t) = v_i(t) + \gamma_i(t) + \tilde{d}_i(x,t)
\end{aligned} \tag{3.13}$$

for $i = 1,2,\cdots,m$. The assumption about the number of inputs p being equal to the number of outputs m must be retained as in Section 3.1 for the existence of a feedback linearization control u. The components $(\tilde{d}_1, \tilde{d}_2, \ldots)$ represent the transformed effects of the unknown inputs and can be obtained as follows [40]:

$$\begin{bmatrix} \tilde{d}_1(x,t) \\ \vdots \\ \tilde{d}_m(x,t) \end{bmatrix} = \begin{bmatrix} L_{Ed}^{r_1-1} h_1 + \ldots + \frac{\mathrm{d}}{\mathrm{dt}}^{(r_1-1)} (L_{Ed} h_1) \\ \vdots \\ L_{Ed}^{r_m-1} h_m + \ldots + \frac{\mathrm{d}}{\mathrm{dt}}^{(r_m-1)} (L_{Ed} h_m) \end{bmatrix} \tag{3.14}$$

The state space canonical form can be written for each subsystem from the transformed

model (3.13) on the basis of (3.9):

$$\begin{aligned}\dot{Z}^i(t) &= A_i Z^i(t) + B_i v_i(t) + M_i \gamma_i(t) + N_i \tilde{d}_i(x,t) \\ y_i(t) &= C_i Z^i(t) + \varpi_i(t)\end{aligned} \tag{3.15}$$

where N_i is an $r_i \times 1$ vector that is identical to M_i.

In order to implement state estimation-based control with the DKF, we apply the standard Kalman filter (3.11) to the linearized model (3.15). However, the DKF is unable to estimate the states of the robot in the presence of unknown inputs. So we need to design a virtual control v_i as in (3.10) using disturbance rejection to stabilize the transformed system dynamics:

$$v_i(t) = Z_{di}^{(r_i)}(t) - \theta_i^T e_i(t) - \hat{\tilde{d}}_i(x,t) \tag{3.16}$$

where $\hat{\tilde{d}}_i(x,t)$ is the estimate of the disturbance / unknown input, which is used for rejection / compensation of the disturbance. We propose two different methods to obtain $\hat{\tilde{d}}_i(x,t)$.

1. Use a PD disturbance compensator as a supervisory control term for the compensation of the disturbance: $\hat{\tilde{d}}_i(x,t) = L_i^T E_i$, with the gain $L_i^T = [L_{Pi}, L_{Di}]$.

2. Use a PI disturbance compensator as a supervisory control term for the compensation of the disturbance: $\hat{\tilde{d}}_i(x,t) = J_i^T \Xi_i$ with $J_i^T = [J_{Pi}, J_{Ii}]$ and $\Xi_i = \left[e_i, \int_0^t e(\tau) d\tau\right]^T$.

The virtual control v_i (3.16) is designed to make the DKF robust to unknown inputs. An augmented system is thus formed on the basis of the DKF for state estimation and the proposed methods for disturbance rejection:

$$\begin{bmatrix} \dot{\hat{Z}}_i(t) \\ \dot{\hat{\tilde{d}}}_i(x,t) \end{bmatrix} = \begin{bmatrix} A_i & N_i \\ 0 & 0 \end{bmatrix} \begin{bmatrix} \hat{Z}_i(t) \\ \hat{\tilde{d}}_i(x,t) \end{bmatrix} + \begin{bmatrix} B_i \\ 0 \end{bmatrix} v_i + \begin{bmatrix} K_i(t)(y(t) - C_i \hat{Z}_i(t)) \\ L_i^T E_i \text{ or } J_i^T \Xi_i \end{bmatrix} \tag{3.17}$$

We define the state estimation errors as $\xi_i(t) = \hat{Z}_i(t) - Z_i(t)$ and the disturbance estimation errors as $\varphi(t) = \hat{\tilde{d}}_i(x,t) - \tilde{d}_i(x,t)$ with $L_{Pi} \gg L_{Di}$ or $J_{Pi} \gg J_{Ii}$. From [40, 60], we can conclude that the estimation error norms $\|\xi_i(s)\|_F$ and $\|\varphi(s)\|_F$ converge to an arbitrarily

small value ε if $\|s\tilde{d}_i(s)\|_F$ is bounded, where $\|\cdot\|_F$ denotes the Frobenius norm and s is the Laplace transform variable. The proposed method for disturbance rejection and the DKF for estimation-based control is depicted in Fig. 10.

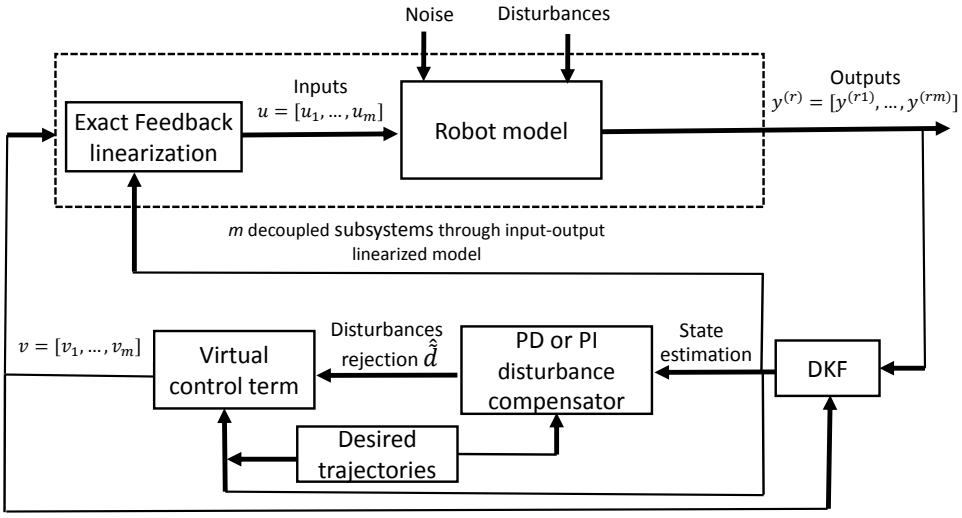

Figure 10: Schematic of the proposed method for disturbance rejection / compensation and the DKF for state estimation-based control of a robotic system

3.3 Simulation Results

In this section we show the effectiveness of the DKF and the robust DKF for state estimation-based control through simulation studies on a three-DOF test robot / prosthesis system. Figure 11 shows a schematic of the hip robot and prosthesis combination. The transfemoral prosthesis and the robot are modeled as a three-link robot. In the robot dynamic model (3.1), the vector of generalized joint displacements is $q = [q_1, q_2, q_3]^T$, where q_1 is vertical hip displacement, q_2 is thigh angle, and q_3 is knee angle. The state vector and outputs of the robot / prosthesis system are given as

$$\mathbf{x} = [q_1, \dot{q_1}, q_2, \dot{q_2}, q_3, \dot{q_3}]^T, \quad y = [q_1, q_2, q_3]^T$$

We thus have three states for the generalized coordinates and three states for their velocities. The inputs $u = [u_1, u_2, u_3]^T$ correspond to the outputs. The input u_i will appear after two

differentiations of the corresponding output y_i, so the total relative degree is obtained from (3.3) as $r = r_1 + r_2 + r_3 = 6$, which is equal to the system order n. Note that there are no internal dynamics associated with the input-output linearization of this system since $r = n$.

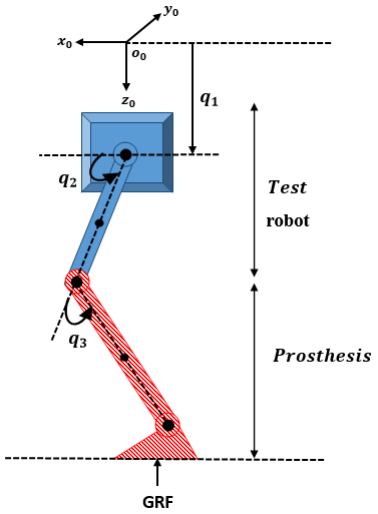

Figure 11: Diagram of the robot / prosthesis system; note that the ankle joint is stationary

Note that (3.1) is trivially input-output linearizable with $u = Ma + C\dot{q} + G$, where a is the virtual acceleration, which results in the system $\ddot{q} = a$. There is no need for output differentiation here, but this system is provided in this thesis as an example to illustrate the combination of the derivative-free Kalman filter and input-output linearization via output differentiation.

First, we assume in Section 3.3.1 that the robot model has known parameters with a known GRF contact model that comprises the external force vector F_e in (3.1). The DKF is designed in this case for state estimation-based control of the robot. Second, we suppose in Section 3.3.2 that the system has unknown external force dynamics and parameter uncertainties, which are treated as unknown inputs. The performance of the robot / prosthesis system is simulated for four steps of normal walking, which is approximately four seconds. A treadmill is used as the walking surface of the prosthesis test robot. The reference data have been provided by the Motion Studies Laboratory of the Cleveland Department of Veterans Affairs Medical Center (VAMC) [34].

3.3.1 The robot / prosthesis system with known inputs

The ground contact model used to simulate $J_e^T F_e$, the generalized joint torques resulting from ground contact in (3.1), is given as follows [5]:

$$L_z = q_1 + l_2 \sin q_2 + l_3 \sin(q_2 + q_3) \tag{3.18}$$

$$F_z = \begin{cases} 0 & \text{if} \quad L_z \leq s_z \\ k_b(L_z - s_z) & \text{if} \quad L_z \geq s_z \end{cases} \tag{3.19}$$

$$F_x = \beta F_z \tag{3.20}$$

$$J_e^T F_e = \begin{bmatrix} F_z \\ F_z(l_3 \cos(q_2 + q_3) + l_2 \cos q_2) - F_x(l_3 \sin(q_2 + q_3) + l_2 \sin q_2) \\ F_z l_3 \cos(q_2 + q_3) - F_x l_3 \sin(q_2 + q_3) \end{bmatrix} \tag{3.21}$$

where $l_2 = 0.425$ m and $l_3 = 0.527$ m are the length of the thigh and shank respectively; L_z is the vertical position of bottom of the foot in the world frame (x_0, y_0, z_0); $s_z = 0.905$ m is the treadmill standoff (that is, the vertical distance from the origin of the world frame to the treadmill); $k_b = 37{,}000$ N/m is the belt stiffness; and $\beta = 0.2$ is the friction coefficient between the foot and the treadmill. The robot dynamics (3.2) is input-output linearized based on the assumption that the number of inputs is equal to the number of outputs. The model is transformed into the three decoupled subsystems

$$\begin{aligned} \dot{Z}_i(t) &= \begin{bmatrix} 0 & 1 \\ 0 & 0 \end{bmatrix} Z_i(t) + \begin{bmatrix} 0 \\ 1 \end{bmatrix} v_i + \begin{bmatrix} 0 \\ 1 \end{bmatrix} \gamma_i(t) \\ y_i(t) &= \begin{bmatrix} 1 & 0 \end{bmatrix} Z_i(t) + \varpi_i(t) \end{aligned} \tag{3.22}$$

where $Z_i(t) = [q_i, \dot{q}_i]^T$ for $i = 1, 2, 3$. We apply the DKF to each linearized subsystem (3.22) to achieve estimation-based control of the robot. The covariance of the process and measurement noise are taken as $Q_i = 5 \times 10^{-3}$ and $R_i = 10^{-3}$ for each subsystem. The measurement noise covariance is based on our knowledge of the accuracy of the measure-

ment system. The process noise covariance is a tuning parameter that is set by trial and error to obtain good estimation and control performance.

The initial value of the state vectors are given as

$$Z_1(0) = [0.019, 0.093]^T \tag{3.23}$$

$$Z_2(0) = [1.131, 0.779]^T \tag{3.24}$$

$$Z_3(0) = [0.092, 1.412]^T \tag{3.25}$$

We set the initial value of the estimated state vector to provide an arbitrary but nonzero initial estimation error:

$$\hat{Z}_1(0) = [0.039, 0.062]^T \tag{3.26}$$

$$\hat{Z}_2(0) = [0.912, 0.321]^T \tag{3.27}$$

$$\hat{Z}_3(0) = [0.135, 0.884]^T \tag{3.28}$$

The gains θ_i in (3.10) are designed by pole placement to provide good control performance: $\theta_i^T = [1250, 100]$ for $i = 1, 2, 3$.

The results for the state estimation-based control of the robot / prosthesis system are shown in Fig. 12. In spite of significant initial estimation errors for the joint coordinates and velocities, the DKF estimates converge quickly to the true states. The control magnitudes are shown in Fig. 13 and are greater than those exerted by able-bodied walkers [16] because the robot dynamics are much different than human dynamics, and the GRF input does not come from human walking. However, implementing the DKF-based controller in the real-world robot / prosthesis would not be a problem. The control signals in this simulation are orders of magnitude closer to able-bodied controls than the nonlinear control method proposed in [16].

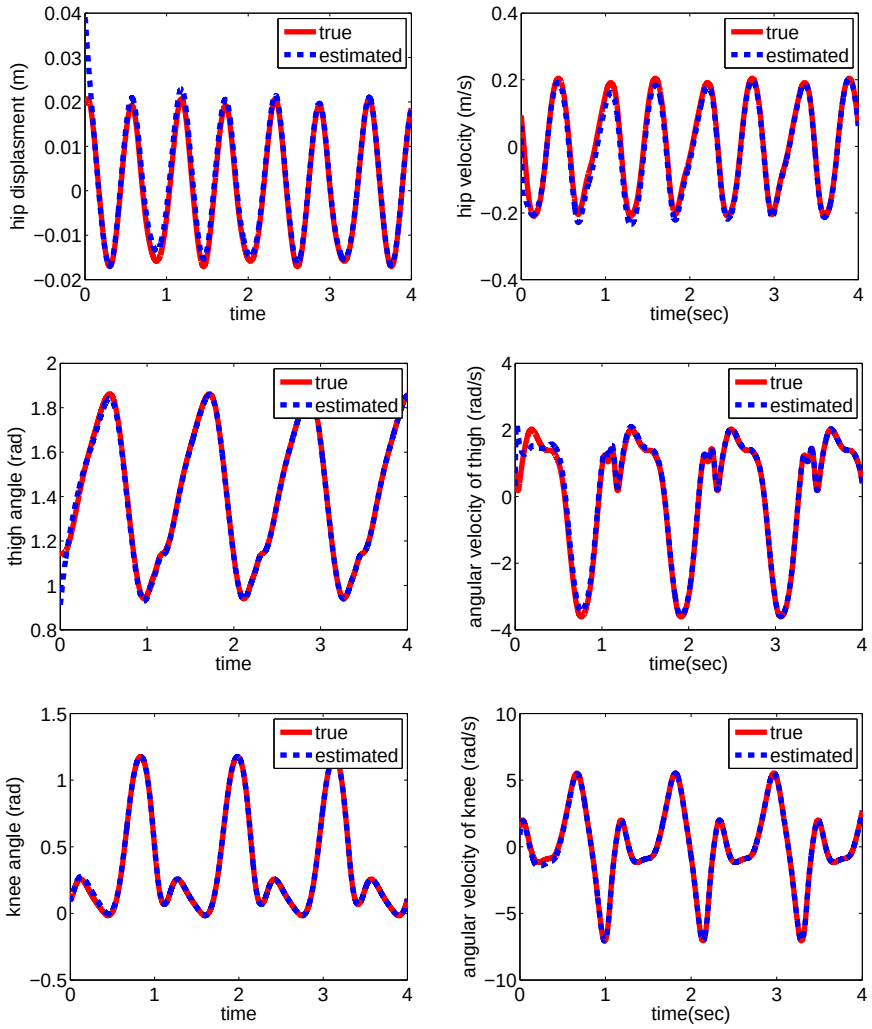

Figure 12: State estimation-based control of the robot / prosthesis system with known inputs: state estimation performance

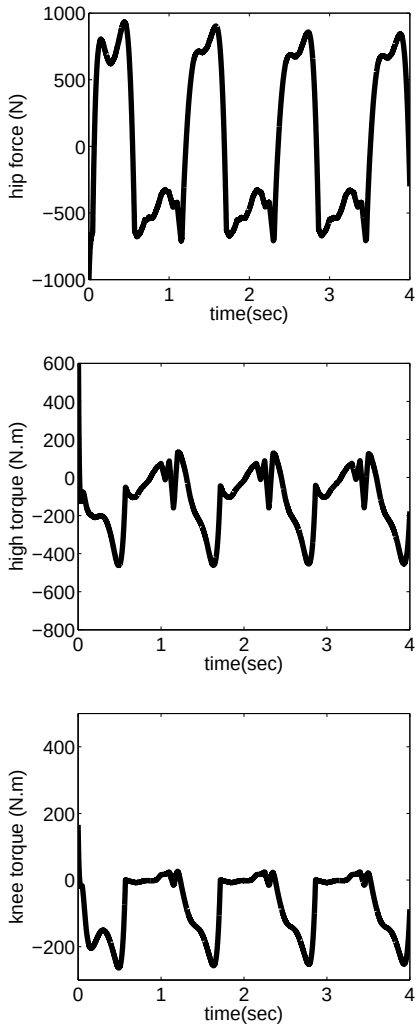

Figure 13: State estimation-based control of the robot / prosthesis system with known inputs: control signal magnitudes

3.3.2 The robot / prosthesis system with unknown inputs

In robot / prosthesis systems, the system parameters may be unknown or may change from their nominal values. Also, external forces F_e, including unmodeled ground reaction forces (GRFs), can be considered as unknown inputs if sensors to measure them are not available. We consider these two sources of uncertainties as unknown inputs d_1, d_2, d_3 in the robot dynamics. We suppose the unknown inputs are given as $d_1 = 100\sin(10t)$ N, $d_2 = -200$ Nm, and $d_3 = 50\sin(5t + \pi)$ Nm. These inputs affect each robot joint via the linearization of the unknown inputs based on (3.14) and are denoted as $\tilde{d}_1, \tilde{d}_2, \tilde{d}_3$ in the linearized system (3.15). The robot dynamics are transformed into three decoupled subsystems on the basis of (3.15). The DKF is designed using the disturbance / unknown input rejection methods proposed in Section 3.2. The values of the initial state vector, estimates, and covariances of the noise terms are identical to those in Section 3.3.1. We use the PD and PI compensators for disturbance rejection via estimation of $\tilde{d}$. The accuracy of the disturbance estimate $\hat{\tilde{d}}$ is compared for the PD and the PI compensators.

First we consider the PD compensator as the supervisory controller for unknown input rejection. We do not show tracking performance since it is very similar to that in the previous subsection. Figure 14 shows good state estimation in spite of significant initialization errors. Figure 15 shows control signals that are approximately equal to those in the previous subsection in spite of the unknown inputs. Figure 16 shows good unknown input estimation as an extra benefit of the DKF approach.

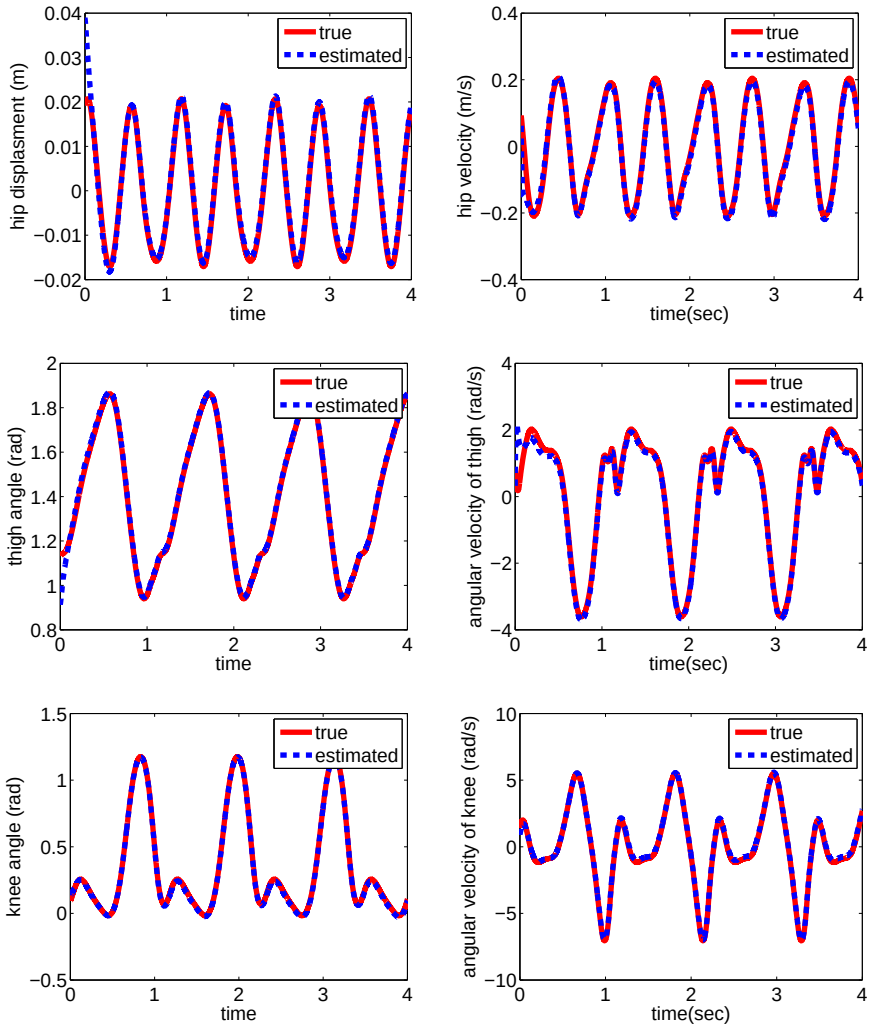

Figure 14: State estimation-based control of the robot / prosthesis system with unknown inputs: state estimation performance with PD compensation

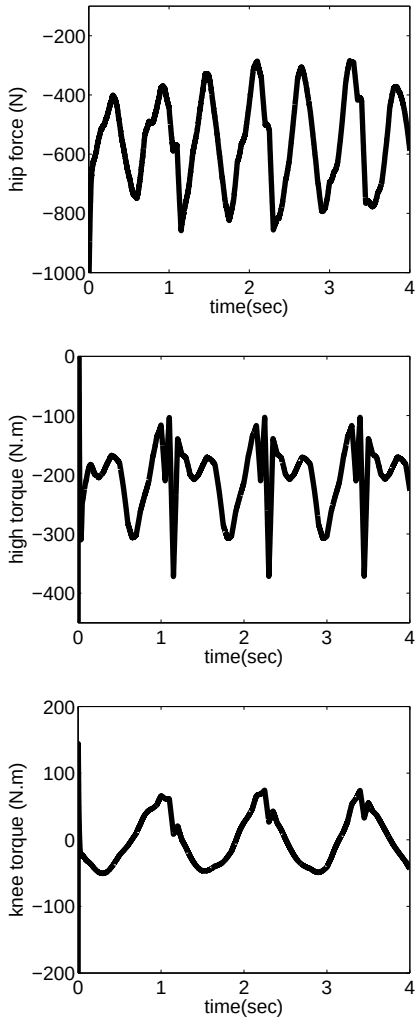

Figure 15: State estimation-based control of the robot / prosthesis system with unknown inputs: control signal magnitudes with PD compensation

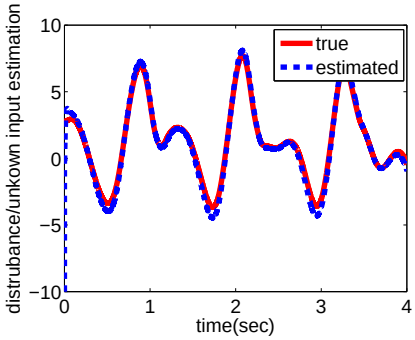

(a) $\hat{\tilde{d}}_1$ (N)

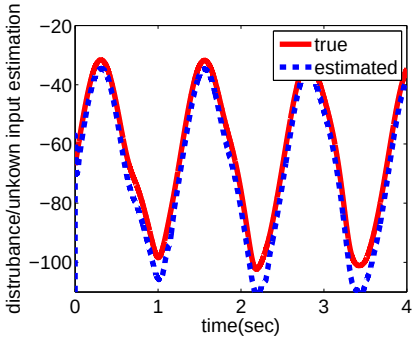

(b) $\hat{\tilde{d}}_2$ (Nm)

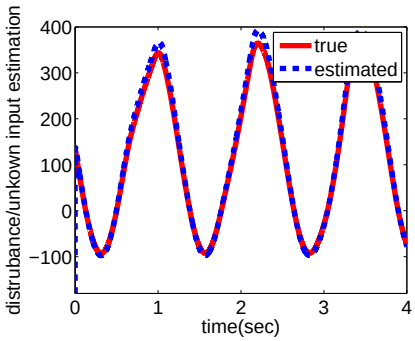

(c) $\hat{\tilde{d}}_3$ (Nm)

Figure 16: State estimation-based control of the robot / prosthesis system with unknown inputs: unknown input estimation with PD compensation

Next we use the PI compensator for unknown input rejection. We do not show tracking performance, state estimation performance, or control signal magnitudes, because they are very similar to those obtained with the PD compensator. Figure 17 shows unknown input estimation, which may be satisfactory depending on the system requirements, but is noticeably worse than than obtained with the PD compensator.

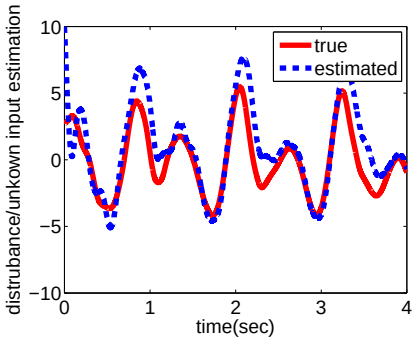

(a) $\hat{\tilde{d}}_1$ (N)

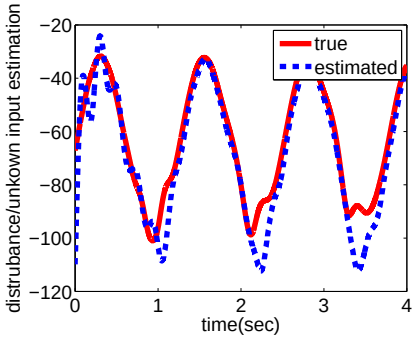

(b) $\hat{\tilde{d}}_2$ (Nm)

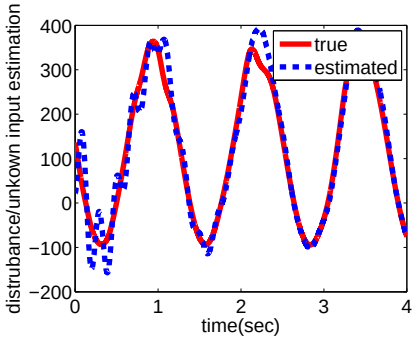

(c) $\hat{\tilde{d}}_3$ (Nm)

Figure 17: State estimation-based control of the robot / prosthesis system with unknown inputs: unknown input estimation with PI compensation

We compare the PD and PI compensators in terms of trajectory tracking root mean square error (RMSE) and RMS control values. Table I shows that the PD compensator outperforms the PI compensator from the following perspectives. (i) The PD compensator has faster dynamics than the PI compensator due to the error derivative term $\dot{e}$; therefore it includes a prediction characteristic that improves compensator response time to the disturbance / unknown input. (ii) The integral term in the PI compensator introduces a pole at the origin. This results in overshoot during transients and also might cause the system to be slow in tracking the desired trajectory. In other words, since the system was linearized based on feedback linearization, a pole at the origin may cause oscillation and reduce stability.

Table I: Comparison of trajectory tracking RMSE and RMS control values of the robust DKF using PD disturbance compensation and PI disturbance compensation

	$\mathbf{x}_1$ **(m)**	$\mathbf{x}_2$ **(m/s)**	$\mathbf{x}_3$ **(rad)**	$\mathbf{x}_4$ **(rad/s)**	$\mathbf{x}_5$ **(rad)**	$\mathbf{x}_6$ **(rad/s)**	$\mathbf{u}_1$ **(N)**	$\mathbf{u}_2$ **(Nm)**	$\mathbf{u}_3$ **(Nm)**
PD compensator	0.001	0.019	0.008	0.019	0.211	0.112	583	217	39
PI compensator	0.001	0.030	0.068	0.022	0.359	0.857	580	211	42

3.4 Discussion

We developed and applied a DKF to a class of MIMO robotic systems for estimation-based control. We then proposed two methods for disturbance / unknown input rejection when the robot dynamics are disturbed by parametric uncertainties or unmodeled but bounded external forces. PD and PI disturbance compensators were used as supervisory control terms for disturbance / unknown input rejection, thus making state estimation more robust in the DKF. In the simulation results, a three-DOF robot / prosthesis system for trans-femoral amputees was considered for estimation-based control of the joint displacements and velocities. The results showed that the DKF converges rapidly in terms of both state estimation and trajectory tracking, even with significant initial estimation errors and measurement noise. Additionally, we demonstrated the robustness of the state estimation-based controller in the presence of unknown inputs. We showed that the DKF achieves smaller estimation errors when the PD compensator is employed for disturbance / unknown input rejection / compensation, relative to the PI compensator. In the next chapter the stability of observer-based robot / prosthesis controller will be discussed and analyzed.

CHAPTER IV

STABILITY ANALYSIS

This chapter discusses stability analysis for nonlinear systems. It begins with a short introduction to the concept of stability for nonlinear systems, including stability types and definitions. Next, it introduces Lyapunov theorems (linearization and direct methods) and invariant set theorems. It then discusses stability analysis of linear systems using Lyapunov functions, along with stability analysis of non-autonomous time-varying systems. Finally, Section 4.7, which comprises the original contribution of this chapter, develops a stability analysis of the DKF method from Chapter III in the frequency domain, and demonstrates error convergence in the time domain.

4.1 Stability in Nonlinear Systems

This section reviews some basic stability concepts for nonlinear systems. An autonomous system, or time-invariant system, is denoted as

$$\dot{x} = f(x) \tag{4.1}$$

A non-autonomous system, or time-varying system, is denoted as

$$\dot{x} = f(x,t) \tag{4.2}$$

When a time-invariant system has a control-input u, the system is denoted as

$$\dot{x} = g(x,u) \tag{4.3}$$

If u is a function of the state x, then the closed-loop representation of the system is denoted as

$$\dot{x} = g(x,u(x)) \tag{4.4}$$

A non-autonomous system with $u = u(x,t)$ is represented as

$$\dot{x} = g(x,u(x,t)) \tag{4.5}$$

An equilibrium point for an autonomous system is defined as a state value x_{eq} such that if $x = x_{eq}$ at some time t_0, then $x = x_{eq}$ for all $t \geq t_0$; that is, $f(x_{eq}) = 0$ for all $t \geq 0$.

As an example, consider a simple pendulum:

$$mr^2\ddot{\theta} + b\dot{\theta} + mgr\,sin(\theta) = 0 \tag{4.6}$$

where θ represents the rotation angle of the pendulum. This system has many equilibrium points: ($\theta = k\pi$, $\dot{\theta} = 0$) for $k = 0, \pm 1, \pm 2, ...$

4.2 Lyapunov Stability

This section defines various types of stability and associated concepts.

4.2.1 Stable Equilibrium Point

$x_{eq} = 0$ is said to be an equilibrium point if, $\forall R > 0$, $\exists r > 0$ such that if $\|x(t_0)\| < r$ then for every $t \geq t_0$, $\|x(t)\| < R$. If the system begins close enough to the equilibrium condition x_{eq} (inside a ball of radius r), it never leaves the ball of radius R.

4.2.2 Local Asymptotic Stability

Suppose there exists an equilibrium point that is stable. It is locally asymptotically stable if $\exists\ r > 0$ such that $\|x(0)\| < r \Rightarrow x(t) \to 0$ as $t \to \infty$.

4.2.3 Global Asymptotic Stability

Suppose there exists an equilibrium point that is stable. It is globally asymptotically stable if, for any initial condition $x(0)$, $x(t) \to 0$ as $t \to \infty$. That is, any initial state returns to the equilibrium point. In this case there exists exactly one equilibrium point $x_{eq} = 0$, and so there is no need to define a region of attraction.

4.2.4 Local Exponential Stability

Suppose there exists an equilibrium point that is stable. It is locally exponentially stable if $\exists\ r > 0$ such that $\|x(0)\| < r \Rightarrow \exists\ \alpha > 0$ and $\lambda > 0$ such that $\|x(t)\| < \alpha\|x(0)\|e^{-(\lambda t)}\ \forall\ t \geq 0$.

4.2.5 Global Exponential Stability

Suppose there exists an equilibrium point that is stable. It is globally exponentially stable if, for any initial condition $x(0)$, $\exists\ \alpha > 0$ and $\lambda > 0$ such that $\|x(t)\| < \alpha\|x(0)\|e^{-(\lambda t)}\ \forall\ t \geq 0$.

With this kind of stability, the time-constant λ indicates how long it takes the trajectory to reach the equilibrium point. Furthermore, if we choose $\alpha = e^{(\lambda T_0)}$ then

$\|x(t)\| < \|x(0)\|e^{-\lambda(t-T_0)}$. As a special case, a linear system is globally exponentially stable if all of its closed-loop poles are in the left-half plane.

4.3 Lyapunov Theorems

Before introducing the Lyapunov theorems, we briefly discuss linearization and local stability.

4.3.1 Linearization and Local Stability

Consider an autonomous nonlinear system:

$$\dot{x} = f(x) \tag{4.7}$$

Suppose this system has an equilibrium point at $x_{eq} = 0$. A Taylor series expansion of $f(x)$ around the origin can be written as

$$\dot{x} = f(0) + \left.\frac{\partial f}{\partial x}\right|_{x=0} x + h.o.t \tag{4.8}$$

where *h.o.t* denotes higher order terms. So the linearized system dynamics can be approximated as

$$\dot{x} \backsimeq Ax \tag{4.9}$$

where the system matrix $A=\left.\frac{\partial f}{\partial x}\right|_{x=0}$, also called the Jacobian matrix, can be written as

$$\frac{\partial f}{\partial x} = \begin{bmatrix} \frac{\partial f_1}{\partial x_1} & \frac{\partial f_1}{\partial x_2} & \cdots & \frac{\partial f_1}{\partial x_n} \\ \frac{\partial f_2}{\partial x_1} & \frac{\partial f_2}{\partial x_2} & \cdots & \frac{\partial f_2}{\partial x_n} \\ \vdots & \vdots & \ddots & \vdots \\ \frac{\partial f_n}{\partial x_1} & \frac{\partial f_n}{\partial x_2} & \cdots & \frac{\partial f_n}{\partial x_n} \end{bmatrix} \tag{4.10}$$

This approach can be generalized to the linearization of a closed-loop system. Consider the nonlinear system

$$\dot{x} = f(x,u) \tag{4.11}$$

Suppose this system has an equilibrium point at $(x,u) = (0,0)$ so that $f(0,0) = 0$. A Taylor series expansion of $f(x,u)$ can be written as

$$\dot{x} = f(0,0) + \left.\frac{\partial f}{\partial x}\right|_{x=0,u=0} x + \left.\frac{\partial f}{\partial x}\right|_{x=0,u=0} u + h.o.t \tag{4.12}$$

Suppose that a controller is implemented so that u is a function of the state x; that is, $u(x) = g(x)$. The Taylor series expansion of u is written as

$$u(x) = g(x) = 0 + \left.\frac{\partial g}{\partial x}\right|_{x=0} x + h.o.t \tag{4.13}$$

So $\dot{x}$ can be approximated as

$$\dot{x} \backsimeq (A + BG)x \tag{4.14}$$

where

$$A = \left.\frac{\partial f}{\partial x}\right|_{x=0,u=0}$$

$$B = \left.\frac{\partial f}{\partial x}\right|_{x=0,u=0}$$

$$G = \left.\frac{\partial g}{\partial x}\right|_{x=0,u=0}$$

As a simple example, suppose that

$$\dot{x_1} = {x_2}^3 + x_1 \cos(x_2) \tag{4.15}$$

$$\dot{x_2} = 2x_2 + (x_1 + 5)x_1 + x_2 \sin(x_1) \tag{4.16}$$

which has an equilibrium point at $(x_1, x_2) = (0, 0)$. The system matrix A can be calculated as

$$A = \begin{bmatrix} 1 & 0 \\ 5 & 2 \end{bmatrix}$$

4.3.2 Lyapunov Linearization and Stability

Here we present a theorem that is important for linear systems and that we will need to use later in our stability proof of the DKF.

Theorem IV.1 *Suppose there exists a nonlinear system such that $\dot{x} = f(x)$ with an equilibrium point at origin; that is, $f(0) = 0$. Suppose that its linearized model is given as $\dot{x} \backsimeq Ax$. The system matrix A can indicate one of several types of stability.*
First, if A is strictly unstable (that is, at least one eigenvalue or closed-loop pole is located in the right-half plane), then $x = 0$ is unstable; that is, it is not stable in the Lyapunov sense.
Second, if A is strictly stable (that is, all eigenvalues or closed-loop poles are located in the left-half plane), then $x = 0$ is asymptotically stable.
Third, if A is marginally unstable (that is, some eigenvalues are on the imaginary axis and others are in the left-half plane), then no conclusion can be made about the stability of the system; it may or may not be stable.

As a simple example, consider the nonlinear system $\dot{v} + v|v| = 0$. Then $\dot{v} = 0$ is the linearized system and satisfies the third condition above. If v is positive then $\dot{v}$ is negative, and if v is negative then $\dot{v}$ is positive, so the linearized system is asymptotically stable in spite of the fact that it has an eigenvalue on the imaginary axis.

4.3.3 Lyapunov's Direct Method

Lyapunov's direct method is based on two simple concepts: *first*, every physical element has finite energy, and *second*, this energy dissipates due to factors like friction and re-

sistance. Lyapunov's direct method is thus based on simple concepts from physics. The following definitions are fundamental to Lyapunov's direct method.

1. $V(x)$ is positive definite (PD) if $V(0) = 0$ and $V(x) > 0$ for every $x \neq 0$.

2. $V(x)$ is positive semidefinite (PSD) if $V(x) \geq 0$ for every x.

3. $V(x)$ is negative definite (ND) if $V(0) = 0$ and $V(x) < 0$ for every $x \neq 0$.

4. $V(x)$ is negative semidefinite (NSD) if $V(x) \leq 0$ for every x.

5. $V(x)$ is indefinite if it does not satisfy any of the above four criteria.

For example, consider a simple mechanical mass-spring system [59, Chapter 3] with a nonlinear spring and damper.

$$m\ddot{x} + b|\dot{x}|\dot{x} + k_0 x + k_1 x^3 = 0 \tag{4.17}$$

where $b|\dot{x}|\dot{x}$ is viscous friction or drag, and $k_0 x + k_1 x^3$ is a spring term. The variable x represents position, $\dot{x}$ represents velocity, and $\ddot{x}$ represents acceleration. The equilibrium point of this system is

$$\begin{aligned} x = x_{eq} &= 0 \\ \dot{x} = \dot{x}_{eq} &= 0 \end{aligned}$$

The equilibrium point can be represented in two-dimensional state space coordinates, with the horizontal axis representing x and the vertical axis representing the derivative of x. The equilibrium point is at the origin of the state space coordinate system. Consider $V(x)$ as the total mechanical energy of the system (that is, the sum of the potential and kinetic energy).

$$V(x) = \frac{1}{2}m\dot{x}^2 + \int_0^x (k_0\tau + k_1\tau^3)\mathrm{d}\tau = \frac{1}{2}m\dot{x}^2 + \frac{1}{2}k_0 x^2 + \frac{1}{4}k_1 x^4 \tag{4.18}$$

Taking the derivative of energy $V(x)$ with respect to time gives the power dissipation, which shows how the energy changes with time.

$$\begin{aligned}\frac{\mathrm{d}}{\mathrm{dt}}V(x) &= m\dot{x}\ddot{x}+(k_0x+k_1x^3)\dot{x}\\ &= \dot{x}(-b|\dot{x}|\dot{x}-k_0x+k_1x^3)+(k_0x+k_1x^3)\dot{x}\\ &= \dot{x}(-b|\dot{x}|\dot{x})\\ &= -b|\dot{x}|^3\end{aligned}$$

The only element in the system that dissipates power is the damper. If $\frac{\mathrm{d}}{\mathrm{dt}}V(x)=0$ then $\dot{x}=0$, which means that the velocity is changing direction (from positive to negative, or vice versa).

Lyapunov's direct method can be applied to local stability as stated by the following theorem.

Theorem IV.2 *Consider the autonomous system*

$$\dot{x}=f(x) \tag{4.19}$$

with initial condition $x(0)=0$. Assume there exists a smooth scalar function $V(x)$ such that in some state-space region (a ball with radius R) $V(x)$ is PD and $\dot{V}(x)$ is NSD. Then $x=0$ is a stable equilibrium point. If $\dot{V}(x)$ is ND, then $x=0$ is an asymptotically stable equilibrium point.

Lyapunov's direct method can be applied to global stability as stated by the following theorem.

Theorem IV.3 *Consider the autonomous system (4.19). Assume there exists a smooth scalar function $V(x)$ such that for all x in $\mathbb{R}^n$, $V(x)$ is PD, $V(x)\to\infty$ as $\|x\|\to\infty$, and $\dot{V}(x)$ is ND. Then $x=0$ is a globally asymptotically stable equilibrium point.*

For example, consider the nonlinear autonomous system $\dot{x} + f(x) = 0$. Assume that $f(x)$ is a continuous and odd function, meaning that $xf(x) > 0$ for all $x(t) \neq 0$. That is, both x and $f(x)$ have the same sign. This system has an equilibrium point at the origin ($x = \dot{x} = 0$), and since both x and $f(x)$ have the same sign, the equilibrium point is globally asymptotically stable. We can show this with Lyapunov theory by choosing $V(x) = x^2$ as the candidate Lyapunov function.

1. $V(x)$ is PD.
2. As $\|x\| \to \infty$, $V(x) \to \infty$.
3. $\dot{V} = 2x\dot{x} = -2xf(x) < 0$ for all $x \neq 0$, which shows that $\dot{V}$ is ND.
4. Therefore, $x = 0$ is a globally asymptotically stable equilibrium, meaning that for any initial condition, x tends to zero as time tends to infinity.

The selection of a Lyapunov function for a given system is not unique, and the above theorems do not indicate how to choose a Lyapunov function. For example, the following functions are valid Lyapunov functions for the above example:

$V(x) = 2x^2$

$V(x) = x^4$

$V(x) = 2x^2 + x^4$

Even $V(x) = \int_0^x f(y)\mathrm{d}y$ can be used as a Lyapunov function for the above system; in this case we obtain $\dot{V} = f(x)\dot{x} = -f^2(x) < 0$ for all $x \neq 0$.

One difficulty of using Lyapunov theorems is that if $\dot{x} = 0 \Rightarrow \dot{V} = 0$, the NSD Lyapunov function indicates that the system's velocity is zero at the equilibrium point, which means that the velocity is changing direction. In other words, since $\dot{x} = 0$, the fact that $\dot{V} = 0$ does not tell us anything about x. In this case we can see that $x = 0$ is stable but we cannot say anything about the asymptotic stability or global asymptotic stability of the system. This shortcoming led to the development of a richer theory that will be discussed in the next section.

4.4 Invariant Sets

Consider a dynamic system $\dot{x} = f(x)$. A state-space set Ω is said to be an *invariant set* if every state-space trajectory that starts in Ω remains in Ω. Limit cycles and equilibrium points are examples of invariant sets.

Theorem IV.4 *Local Invariant Set Theorem – Consider the autonomous dynamic system $\dot{x} = f(x)$ and the associated Lyapunov function $V(x)$, where:*

1. *$f(x)$ is continuous;*
2. *$V(x)$ is a scalar function of the state x and is bounded for all $x \in \Omega_L$, meaning that $V(x) < L$ for some finite constant L;*
3. *The first derivative of $V(x)$ is continuous;*
4. *Ω_L is bounded;*
5. *$\dot{V} \leq 0$ for all $x \in \Omega_L$.*

Then all trajectories in Ω_L tend to the set R, and more precisely, to the largest invariant set in the set R, which we denote as the set M.

Theorem IV.5 *Global Invariant Set Theorem – Consider the autonomous dynamic system $\dot{x} = f(x)$ and the associated Lyapunov function $V(x)$, where:*

1. *$f(x)$ is continuous;*
2. *$V(x)$ is a scalar function of the state x;*
3. *The first derivative of $V(x)$ is continuous;*
4. *$V(x) \to \infty$ as $\|x\| \to \infty$;*
5. *$\dot{V}(x) \leq 0$ for all x.*

Let R be the set of all points such that $\dot{V}(x) = 0$, and let M be the largest invariant set in the set R. Then all trajectories converge to the set M as $t \to \infty$.

4.5 Lyapunov Stability of Linear Systems

In this section we discuss how Lyapunov stability analysis can be applied to linear systems. We first state the following definitions for a constant square matrix P.

1. P is symmetric if $P^T = P$.

2. P is skew-symmetric if $P^T = -P$.

So any matrix P can be written in the form

$$P = \underbrace{\frac{P+P^T}{2}}_{P_{sym}} + \underbrace{\frac{P-P^T}{2}}_{P_{skew}}$$

Suppose P is a skew-symmetric matrix. We can then take an arbitrary vector x and compute the quadratic (which is scalar) as

$$(x^T P x)^T = x^T P^T x = -x^T P x \tag{4.20}$$

which implies that $x^T P x = 0$ if P is skew-symmetric. This result implies that the quadratic form of any square matrix is:

$$x^T P x = x^T (P_{sym} + P_{skew}) x = x^T P_{sym} x$$

The following symmetry-related properties can be stated.

1. Suppose P is a symmetric matrix that is composed of real elements. Then all of its eigenvalues are real and its eigenvectors can be chosen to be orthonormal; that is, P is diagonizable.

2. A square matrix P is positive definite ($P > 0$) if $x^T P x > 0$ for all $x \neq 0$.

3. If $P > 0$ then $x^T P x$ is a globally positive definite function.

4. $\lambda_{min}(P_{sym})x^T x \leq x^T Px = x^T P_{sym} x \leq \lambda_{max}(P_{sym})x^T x$.

Now we can discuss some concepts that are related to the Lyapunov stability analysis of linear time-invariant systems. Consider the linear time-invariant system $\dot{x} = Ax$. Choose the candidate Lyapunov function $V = x^T Px$, where P is a constant symmetric positive definite matrix ($P = P^T > 0$). Then $V \to \infty$ as $x \to \infty$. Taking the derivative of V with respect to time gives

$$\dot{V} = \dot{x}^T Px + x^T P\dot{x} = \dot{x}^T (A^T P + PA)x$$

In order to show that the system is strictly stable, we need to find a pair of matrices P and Q, both of which are positive definite, to solve the equation $A^T P + PA = -Q$; this is called a Lyapunov equation. The standard approach to solve this equation is to solve for P given a specific Q. That is, given some $Q = Q^T > 0$ (for instance, $Q = I$), find a solution P to the Lyapunov equation. In fact, if the system $\dot{x} = Ax$ is strictly stable, then the solution $P = P^T > 0$ can be written as $P = \int_0^\infty e^{A^T t} Q e^{At} \mathrm{d}t$. This approach can be used to prove the global asymptotic stability of the system.

4.6 Stability Analysis of Non-autonomous Systems

Non-autonomous systems can be either linear or nonlinear systems that vary with time. We discuss both types of systems in this section.

4.6.1 Stability Analysis of Linear Time-Varying Systems

Consider an autonomous dynamic system and the time derivative of a candidate Lyapunov function.

$$\dot{x} = f(x) \tag{4.21}$$

$$\frac{\mathrm{d}}{\mathrm{dt}} V(x) = \frac{\partial V}{\partial x} f(x) = \dot{V}(x) \tag{4.22}$$

Suppose that the system is linear and time-varying:

$$\dot{x}(t) = A(t)x(t) \tag{4.23}$$

It is natural to suppose that if all of the eigenvalues of the system at all points in time are strictly negative, then the system is stable. However, this supposition is false. As a counterexample, consider the system

$$\dot{x} = \begin{bmatrix} -1 & e^{3t} \\ 0 & -1 \end{bmatrix} x \tag{4.24}$$

For this system $\lambda_1 = -2$ and $\lambda_1 = -1$ for all t. However, solving the differential equation for x_2 and substituting it in x_1 gives

$$\dot{x_2} = -x_2 \Rightarrow x_2 = x_2(0)e^{-t} \tag{4.25}$$

$$\dot{x_1} + x_1 = e^{3t}x_2 = e^{3t}x_2(0)e^{-t} = x_2(0)e^{2t} \tag{4.26}$$

We see that $x_2 \to 0$ as $t \to \infty$. However, $x_1 \to \infty$ as $t \to \infty$.

Theorem IV.6 *Given a linear time-varying system $\dot{x}(t) = A(t)x(t)$, if all eigenvalues of $A_{sym} = \frac{A+A^T}{2}$ are less than $-\lambda$ (where λ is a constant positive real value) for all $t > 0$, then $x(t) \to 0$ exponentially at the rate λ.*

Proof. Let $V = x^T x$; then

$$\dot{V} = \dot{x}^T x + x^T \dot{x} = x^T (A^T + A)x \leq -2\lambda x^T x = -2\lambda V$$

$$\dot{V} + 2\lambda V \leq 0 \Rightarrow 0 \leq V \leq V_{(t=0)}e^{-2\lambda t}$$

Since V tends to zero exponentially at the rate 2λ, we conclude that $x(t)$ decreases expo-

nentially at the rate λ; that is, $x(t) = x(0)e^{-\lambda t}$. ■

4.6.2 Stability Analysis of Nonlinear Time-Varying Systems

Before introducing a stability theorem for nonlinear time-varying systems, we make some assumptions and then we justify them.

First, suppose that $\dot{f}(t) \to 0$ as $t \to \infty$. Does this imply that $f(t)$ converges to a limit as $t \to \infty$? Consider the counterexample $f(t) = \log(t)$. It is clear that $\dot{f}(t) \to 0$ as $t \to \infty$. However, $f(t) \to \infty$ as $t \to \infty$. Consider the function $f(t) = \sin(\log(t))$. Then $\dot{f}(t) = \frac{1}{t}\cos(\log(t))$, and so $\dot{f}(t) \to 0$. Although it is true that $-1 \leq f(t) \leq 1$, the function $f(t)$ does not converge to a limit as $t \to \infty$.

Second, suppose that $f(t)$ converges to a finite limit as $t \to \infty$. Does this imply that $\dot{f}(t) \to 0$ as $t \to \infty$? Consider the counterexample $f(t) = e^{-t}\sin(e^{2t})$. The first derivative has the form $\dot{f}(t) = \cdots + e^{t}(\cdots)$, showing that $\dot{f}(t)$ does not converge to 0 as $t \to \infty$.

Third, suppose that $f(t)$ is a lower bounded function whose derivative satisfies $\dot{f}(t) \leq 0$. Does this imply that $f(t)$ tends to a finite limit as $t \to \infty$? This question is answered in the following.

Lemma IV.1 *Barbalat's Lemma Suppose that: (1) There is a scalar function $f(t)$ that tends to a finite limit as $t \to \infty$; (2) Its second derivative is bounded, meaning that $\exists\, \beta > 0$ such that $|\ddot{f}(t)| \leq \beta$. Then $\dot{f}(t) \to 0$ as $t \to \infty$.*

Theorem IV.7 *Consider a non-autonomous system with the dynamics*

$$\dot{x} = f(x,t) \tag{4.27}$$

Suppose that: (1) There exists a Lyapunov-like function $V(x,t)$ that is lower bounded; (2) $\frac{d}{dt}V \leq 0$ for all t; (3) $\frac{d^2}{dt}V$ is bounded. Then $\frac{d}{dt}V \to 0$ as $t \to \infty$.

V is often chosen such that $\dot{V} = -e^2$, where e denotes a trajectory tracking error (if the system under consideration is a control system) or estimation error (if the system under consideration is a state estimator). In this case, the application of Lyapunov theory and the demonstration that $\dot{V} \to 0$ shows that the error tends to zero.

4.7 Stability Analysis of Derivative-Free Kalman Filter

In this section we analyze the stability of the proposed DKF method from Chapter III. We first derive the dynamics $\dot{e}_i(t)$ of the state estimation error and the dynamics $\dot{\phi}_i(t)$ of the unknown input estimation error. We then use a Laplace transform approach for a frequency domain analysis of the transfer functions of the two estimation errors. Additionally, a time domain analysis is used to demonstrate convergence. Finally, a theorem is presented to conclude the discussion of DKF stability.

4.7.1 Error Dynamics

Recall from Chapter III that feedback linearization was used to transform the original robotic system dynamics to a new coordinate system, resulting in m decoupled subsystems as shown in (3.7):

$$\begin{aligned} \dot{Z}_1^i(t) &= Z_2^i(t) \\ &\vdots \\ \dot{Z}_{r_i}^i(t) &= y_i^{(r_i)}(t) = v_i(t) + \gamma_i(t) \end{aligned} \tag{4.28}$$

for $i = 1,2,\ldots,m$. This transformed model can be expressed in state space canonical form as

$$\begin{bmatrix} \dot{Z}_1^i(t) \\ \dot{Z}_2^i(t) \\ \vdots \\ \dot{Z}_{r_i}^i(t) \end{bmatrix} = \overbrace{\begin{bmatrix} 0 & 1 & \cdots & 0 \\ \vdots & 0 & \ddots & 0 \\ 0 & \cdots & 0 & 1 \\ 0 & \cdots & \cdots & 0 \end{bmatrix}}^{A_i} \begin{bmatrix} Z_1^i(t) \\ Z_2^i(t) \\ \vdots \\ Z_{r_i}^i(t) \end{bmatrix} + \overbrace{\begin{bmatrix} 0 \\ 0 \\ \vdots \\ 1 \end{bmatrix}}^{B_i} v_i(t) + \overbrace{\begin{bmatrix} 0 \\ 0 \\ \vdots \\ 1 \end{bmatrix}}^{M_i} \gamma_i(t)$$

$$y_i(t) = \underbrace{\begin{bmatrix} 1 & 0 & \cdots & 0 \end{bmatrix}}_{C_i} Z_i(t) + \varpi_i(t) \tag{4.29}$$

for $i = 1,2,\ldots,m$, or in more compact notation as

$$\begin{aligned} \dot{Z}^i(t) &= A_i Z^i(t) + B_i v_i(t) + M_i \gamma_i(t) \\ y_i(t) &= C_i Z^i(t) + \varpi_i(t) \end{aligned} \tag{4.30}$$

for $i = 1,2,\ldots,m$. The form of (A_i, B_i) and (A_i, C_i) shows that the linearized system is fully controllable and observable for each $i = 1,2,\ldots,m$. The observer equations are given from Chapter III as

$$\begin{aligned} \hat{Z}_i(0) &= E[Z_i(0)] \\ P_i(0) &= E\left[\left(Z_i(0) - \hat{Z}_i(0)\right)\left(Z_i(0) - \hat{Z}_i(0)\right)^T\right] \\ K_i(t) &= P_i(t) C_i^T R_i^{-1}(t) \\ \dot{\hat{Z}}_i(t) &= A_i \hat{Z}_i(t) + B_i v_i(t) + K_i(t)(y_i(t) - C_i \hat{Z}_i(t)) \\ \dot{P}_i(t) &= A_i P_i(t) + P_i(t) A_i^T(t) + Q_i(t) - P_i(t) C_i^T R_i^{-1}(t) C_i P_i(t) \end{aligned} \tag{4.31}$$

for $i = 1,2,\ldots,m$, where $K_i(t)$ and $P_i(t)$ are the Kalman gain and estimation error covariance matrix, and the covariances of the process and measurement noise are $Q_i(t) =$

$E\left[\gamma_i(t)\gamma_i^T(t)\right]$ and $R_i(t) = E\left[\varpi_i(t)\varpi_i^T(t)\right]$, respectively.

In order to analyze the stability of the closed-loop system, we need to formulate the dynamics of the estimation error and the unknown input error. These equations of the system and observer models in the presence of unknown inputs were introduced in Chapter III but are restated here for ease of reference. From (4.29) the system models with unknown input are given as

$$\begin{aligned} \dot{Z}_i(t) &= A_i Z_i(t) + B_i v_i(t) + M_i \gamma_i(t) + N_i \tilde{d}_i(x,t) \\ y_i(t) &= C_i Z^i(t) + \varpi_i(t) \end{aligned} \tag{4.32}$$

for $i = 1,2,\ldots,m$, where N_i is an $r_i \times 1$ vector that is identical to M_i. From (4.32) the observer models are given as

$$\begin{aligned} \dot{\hat{Z}}_i(t) &= A_i \hat{Z}_i(t) + B_i v_i(t) + N_i \hat{\tilde{d}}_i(x,t) + K_i(t)(y_i(t) - C_i \hat{Z}_i(t)) \\ \hat{y}_i &= C_i \hat{Z}_i(t) \end{aligned} \tag{4.33}$$

for $i = 1,2,\ldots,m$. Define the following estimation errors:

$$e_i(t) = \hat{Z}_i(t) - Z_i(t) \tag{4.34}$$

$$\phi_i(t) = \hat{\tilde{d}}_i(x,t) - \tilde{d}_i(x,t) \tag{4.35}$$

$e_i(t)$ is the state estimation error, and $\phi_i(t)$ is the unknown input estimation error, both defined in the transformed (linearized) coordinate system. The error dynamics can then be written as

$$\begin{aligned} \dot{\hat{Z}}_i(t) - \dot{Z}_i(t) =& A_i(\hat{Z}_i(t) - Z_i(t)) + N_i(\hat{\tilde{d}}_i(x,t) - \tilde{d}_i(x,t)) - \\ & K_i C_i(\hat{Z}_i(t) - Z_i(t)) + K_i \varpi(t) - M_i \gamma_i(t) \end{aligned} \tag{4.36}$$

$$\dot{e}_i(t) = (A_i - K_i C_i)e_i(t) + N_i\phi(t) + K_i\varpi_i(t) - M_i\gamma_i(t) \tag{4.37}$$

Recall from (3.17) that

$$\hat{\dot{d}}_i(x,t) = \Psi_i(\hat{y}_i(t) - y_i(t)) \tag{4.38}$$

Substituting for y_i and $\hat{y}_i$ from (4.32) and (4.33) respectively gives

$$\hat{\dot{d}}_i(x,t) = \Psi_i C_i[(\hat{Z}_i(t) - Z_i(t))] - \Psi_i\varpi_i(t) \tag{4.39}$$

where Ψ_i is a large positive value whose exact value depends on whether PD or PI compensation is used. The first derivative of $\phi_i(t)$ (defined above) gives

$$\dot{\phi}_i(t) = \Psi_i C_i[\dot{e}_i(t)] - \Psi_i\dot{\varpi}_i(t) - \ddot{\hat{d}}_i(t) \tag{4.40}$$

Substituting $\dot{e}_i(t)$ from (4.37) gives

$$\begin{aligned}\dot{\phi}_i(t) =& \Psi_i C_i[(A_i - K_i C_i)e_i(t) + N_i\phi(t) + K_i(\varpi_i(t)) - M_i\gamma_i(t)] - \Psi_i\dot{\varpi}_i(t) - \ddot{\hat{d}}_i(t) + \\ & [\Psi_i C_i(A_i - K_i C_i)]e_i(t) + [\Psi_i C_i N_i]\phi_i(t) + [\Psi_i C_i K_i]\varpi_i(t) - [\Psi_i C_i M_i]\gamma_i(t) - \\ & \Psi_i\dot{\varpi}_i(t) - \ddot{\hat{d}}_i(t)\end{aligned} \tag{4.41}$$

Recall from Chapter III that $\gamma_i(t)$ is the sum of the process noise $\omega_i(t)$ and the $r_i{}^{th}$ derivative of the measurement noise $\frac{\mathrm{d}}{\mathrm{dt}}^{r_i}\varpi_i(t)$:

$$\gamma_i\,(t) = \omega_i(t) + \frac{\mathrm{d}}{\mathrm{dt}}^{r_i}\varpi_i(t) \tag{4.42}$$

where r_i is the smallest integer such that at least one of the inputs u_i appears in $y_i^{(r_i)}$. Substituting (4.42) into (4.41) and (4.37) gives the final form of the estimation error dynamics:

$$\dot{e}_i(t) = (A_i - K_i C_i)e_i(t) + N_i\phi(t) + K_i\varpi_i(t) - M_i\omega_i(t) - M_i\frac{\mathrm{d}}{\mathrm{dt}}^{r_i}\varpi_i(t) \tag{4.43}$$

$$\dot{\phi}_i(t) = [\Psi_i C_i(A_i - K_i C_i)]e_i(t) + [\Psi_i C_i N_i]\phi_i(t) + [\Psi_i C_i K_i]\varpi_i(t)$$
$$-[\Psi_i C_i M_i]\omega_i(t) - [\Psi_i C_i M_i]\frac{\mathrm{d}}{\mathrm{dt}}^{r_i}\varpi_i(t) - \Psi_i\dot{\varpi}_i(t) - \dot{\tilde{d}}_i(t) \tag{4.44}$$

These equations can be useful in improving the estimator and controller designs. First, it can be seen that there is a mutual relationship between state estimation error and unknown input estimation error, meaning that convergence to a bound will be mutual. This issue will be addressed in detail in the following. Second, for both dynamic equations, we can identify parameters or factors that have major or minor roles in stabilization. To address this second point in more detail, we will take the Laplace transforms and find the transfer functions of each estimation error with respect to each factor. We define the following matrices for ease of notation.

$$M_{1i} = \Psi_i C_i(A_i - K_i C_i) \tag{4.45}$$
$$M_{2i} = \Psi_i C_i N_i \tag{4.46}$$
$$M_{3i} = \Psi_i C_i K_i \tag{4.47}$$
$$M_{4i} = \Psi_i C_i M_i \tag{4.48}$$

The unknown input estimation error dynamics can then be written as

$$\dot{\phi}_i(t) = M_{1i}e_i(t) + M_{2i}\phi_i(t) + M_{3i}\varpi_i(t) - M_{4i}\omega_i(t) - M_{4i}\varpi_i^{r_i}(t) - \Psi_i\dot{\varpi}_i(t) - \dot{\tilde{d}}_i(t) \tag{4.49}$$

The two estimation error dynamics can be combined from (4.43) and (4.49) as

$$\begin{bmatrix} \dot{e}_i(t) \\ \dot{\phi}_i(t) \end{bmatrix} = \begin{bmatrix} A_i - K_i C_i & N_i \\ M_{1i} & M_{2i} \end{bmatrix} \begin{bmatrix} e_i(t) \\ \phi_i(t) \end{bmatrix} + \begin{bmatrix} K_i \\ M_{3i} \end{bmatrix} \varpi_i(t) + \begin{bmatrix} 0 \\ -\Psi_i \end{bmatrix} \dot{\varpi}_i(t)$$
$$+ \begin{bmatrix} -M_i \\ -M_{4i} \end{bmatrix} \varpi_i^{r_i}(t) + \begin{bmatrix} -M_i \\ -M_{4i} \end{bmatrix} \omega_i(t) + \begin{bmatrix} 0 \\ -\dot{\tilde{d}}_i(t) \end{bmatrix} \tag{4.50}$$

This augmented formulation explicitly shows the inter-dependence of the dynamics of the two estimators.

Before proceeding, we need to address two issues: the noise property mentioned in Chapter III, and the assumptions about the two error dynamics.

As (3.17) shows, we need to consider process noise and measurement noise in the i-th subsystem, as well as their derivatives up to order r_i, which is the smallest integer such that at least one of the inputs u_i appears in $y_i^{(r_i)}$. We need to address the issue of why the noise measurement derivative appears in the error dynamics but the process noise derivative does not. We also need to address the properties of the derivatives of the noise.

One of the assumptions for input-output feedback linearization is that the measurement is a linear function of the states. Therefore, applying the derivative operator to the flat output until one of the inputs u_i appears differentiates the measurement noise. Therefore, the noise derivative becomes an input of the transformed system dynamics.

We need to assume that the noises are bandlimited Gaussian noise. This is an easy assumption to satisfy because all noise in physical systems is bandlimited (that is, finite energy). Since differentiation is a linear operator, the derivative of a Gaussian process is a Gaussian process [49]. Therefore, if the mean and covariance of the original Gaussian noise is known, we can calculate the mean and covariance of the differentiated noise.

The process noise is partially due to parameter uncertainties, partially due to unmodeled dynamics, and partially due to input uncertainty. This noise is modeled as an input to the system dynamics, which is a differential equation of order r_i that includes at least one of the inputs u_i, and therefore we do not need to differentiate the process noise in feedback linearization.

For an affine system, feedback linearization results in a canonical form, meaning that the transformed system is fully controllable and observable. The transformed system matrix $A_i - K_i C_i$ is strictly stable for each decoupled subsystem ($i = 1, \cdots, m$). Up to that point in the development it is assumed that there are no unknown inputs and that the system

is noise-free. In that case, (3.17) suggests a stable system for both trajectory tracking and stabilization, and the state tends to equilibrium at the exponential rate $e^{(A-KC)t}$. However, due to the unknown input, the error dynamics above has an additional term $N_i\phi(t)$ that does not allow the error to reach equilibrium.

Additionally, (3.17) shows that the dynamics of the unknown input estimation error not only has a mutual interconnection with the state estimation error dynamics, but also has a relationship with the term $\dot{\tilde{d}}_i(t)$, which is the derivative of the effect of the unknown input on the transformed states. Assume that the unknown input dynamics is noise-free, while $\dot{\tilde{d}}_i(t)$ is still an input to the system. In this case we can expect the estimation errors to converge to unknown but nonzero values. Therefore, $\dot{\tilde{d}}_i(t)$ plays a key role in the error bounds of the estimators. These bounds can be viewed as a physical property of the system and should be considered in the overall system design.

Finally, the previous assumptions about the system being noise-free were made to demonstrate the major factors in stability. In the presence of noise, performance will decrease depending on the magnitude of the noise. This issue will be addressed with a frequency domain analysis.

4.7.2 Laplace Transform of the Error Dynamics

The Laplace transform and frequency domain analysis provide several benefits in control and estimator design.

1. Recall that the system that we are considering is nonlinear. We used feedback linearization to transform the nonlinear system (with actual control input u) to a linear system (with virtual control input v). Therefore, applying linear techniques or operators (the Laplace transform in this section) to the virtual linear system is possible.

2. Consider (3.17) as an extended expression of the error dynamics. It is clear that the dynamics depend not only on the measurement noise (ϖ_i) but also on its derivatives

$(\dot{\varpi}_i(t), ..., \varpi_i^{r_i}(t))$. The Laplace transform provides a method to reduce all of these noise inputs to a single system input, as will be shown in this section.

3. As discussed earlier, the dynamics of the state estimation error and the unknown input estimation error are interconnected. The dynamics include measurement noise and its derivatives. In the time domain, separating them to illustrate their effect on the estimation errors is not mathematically possible; however, the Laplace transform approach provides a way to illustrate their effect on the estimation errors.

4. Superposition theory can be used to define the influence of every independent input on the system, and then to combine their effects as desired.

We take the Laplace transform of (4.43) and (4.49), which are the state estimation and unknown input estimation error dynamics:

$$sE_i(s) = (A_i - K_iC_i)E_i(s) + N_i\Phi_i(s) + K_i\varpi_i(s) - M_i\omega_i(s) - s^{r_i}M_i\varpi_i(s) \tag{4.51}$$

Define $\Gamma_i(s) = [sI - (A_i - K_iC_i)]$ for ease of notation. This matrix has full rank due to the observability of the underlying system, so its inverse exists. We then have

$$E_i(s) = \Gamma_i{}^{-1}(s)N_i\Phi_i(s) + \Gamma_i{}^{-1}(s)[K_i - s^{r_i}M_i]\varpi_i(s) - \Gamma_i{}^{-1}(s)M_i\omega_i(s) \tag{4.52}$$

This gives the transfer function from the unknown input estimation error to the state estimation error, and also from both the process and measurement noise to the state estimation error.

We take the Laplace transform of (4.49) as follows.

$$s\Phi_i(s) = M_{1i}E_i(s) + M_{2i}\Phi_i(s) + [M_{3i} - s^{r_i}M_i - s\Psi_i]\varpi_i(s) - M_{4i}\omega_i(s) - s\tilde{d}_i(s) \tag{4.53}$$

By substituting $E_i(s)$ from (4.52), we obtain

$$[sI - M_{2i} - M_{1i}{\Gamma_i}^{-1}(s)N_i]\Phi_i(s) = (M_{1i}{\Gamma_i}^{-1}(s)[K_i - s^{r_i}M_i] + [M_{3i} - s^{r_i}M_i - s\Psi_i])\varpi_i(s) - [M_{1i}{\Gamma_i}^{-1}(s)M_i + M_{4i}]\omega_i(s) - s\tilde{d}_i(s) \tag{4.54}$$

Define $\Delta_i = [sI - M_{2i} - M_{1i}{\Gamma_i}^{-1}(s)N_i]$ for ease of notation. We then have

$$\begin{aligned}\Phi_i(s) =& {\Delta_i}^{-1}(M_{1i}{\Gamma_i}^{-1}(s)[K_i - s^{r_i}M_i] + [M_{3i} - s^{r_i}M_i - s\Psi_i])\varpi_i(s) - \\ & {\Delta_i}^{-1}[M_{1i}{\Gamma_i}^{-1}(s)M_i + M_{4i}]\omega_i(s) - {\Delta_i}^{-1}s\tilde{d}_i(s)\end{aligned} \tag{4.55}$$

We now have the transfer function from both the process and measurement noise to the unknown input estimation error, as well as the transfer function of the derivative of the unknown input to the unknown input estimation error.

The Laplace transform enables us to separate the contribution of each input to the estimation errors. Now we summarize the transfer functions obtained above.

Transfer functions to state estimation error:

$E_i(s)/\omega_i(s) = -{\Gamma_i}^{-1}(s)M_i$

$E_i(s)/\varpi_i(s) = {\Gamma_i}^{-1}(s)[K_i - s^{r_i}M_i]$

$E_i(s)/\Phi_i(s) = {\Gamma_i}^{-1}(s)N_i$

Transfer functions to unknown input estimation error:

$\Phi_i(s)/\omega_i(s) = -{\Delta_i}^{-1}[M_{1i}{\Gamma_i}^{-1}(s)M_i + M_{4i}]$

$\Phi_i(s)/\varpi_i(s) = {\Delta_i}^{-1}(M_{1i}{\Gamma_i}^{-1}(s)[K_i - s^{r_i}M_i] + [M_{3i} - s^{r_i}M_i - s\Psi_i])$

$\Phi_i(s)/\tilde{d}_i(s) = -{\Delta_i}^{-1}$

We have derived the error dynamics and their state representations. We have begun the frequency domain analysis by taking the Laplace transform of each estimation

error dynamics to obtain the transfer function with respect to each input. Next, we will introduce some assumptions and lemmas regarding these transfer functions.

4.7.3 Assumptions and Bounds

Every physical system has limitations that are generally related to the system's physical properties. To achieve stable and reliable control performance, it is necessary to recognize the system's limitations and constraints. For the robot / prosthesis system, there are several limitations and constraints that facilitate the design and analysis of the estimation / control algorithm.

Condition 1 *The state estimation error* (4.52) *is bounded if:*

1. *The magnitudes of both process noise* $\omega_i(s)$ *and measurement noise* $\varpi_i(s)$ *are sufficiently small and their transfer functions to* $E_i(s)$ *are stable.*

2. $\Phi_i(s)$ *is bounded and differentiable, and its transfer function to* $E_i(s)$ *is stable.*

Condition 2 *The unknown input estimation error* (4.55) *is bounded if:*

1. *The magnitudes of both process noise* $\omega_i(s)$ *and measurement noise* $\varpi_i(s)$ *are sufficiently small and their transfer functions to* $\Phi_i(s)$ *are stable.*

2. *The unknown input* $\tilde{d}(s)$ *is bounded, continuous, and differentiable. In addition,* $s\tilde{d}(s)$ *is bounded and its transfer function to* $\Phi_i(s)$ *is stable.*

Condition 1 can be written as the following conditions that need to be satisfied

for the boundedness of the state estimation error.

$$\|\omega_i(s)\| = \varepsilon_p \|s\tilde{d}(s)\| \leq \|s\tilde{d}(s)\| \tag{4.56}$$

$$\|\varpi_i(s)\| = \varepsilon_m \|s\tilde{d}(s)\| \leq \|s\tilde{d}(s)\| \tag{4.57}$$

$$\|{\Gamma_i}^{-1}(s)M_i\|_\infty \leq \delta p_e \tag{4.58}$$

$$\|{\Gamma_i}^{-1}(s)[K_i - s^{r_i}M_i]\|_\infty \leq \delta m_e \tag{4.59}$$

$$\|{\Gamma_i}^{-1}(s)N_i\|_\infty \leq \eta_{\phi_e} \tag{4.60}$$

where $0 \leq \varepsilon_p, \varepsilon_m \leq 1$ are small positive numbers, and $\|\cdot\|_\infty$ denotes the supremum norm of a transfer function. Both process and measurement noise magnitudes are assumed to be sufficiently small. Additionally, the noise magnitudes and bandwidths should be approximately known. The noise magnitude should be bounded with the derivative of the unknown input $s\tilde{d}(s)$. The quantities δp_e, δm_e, and η_{ϕ_e} are positive numbers that respectively denote the upper bounds of the transfer functions from the process noise, the measurement noise, and the unknown input estimation error, to $E_i(s)$. We can make several observations about the above assumptions.

1. It is reasonable to assume that a noisy system is stable only if the noise-free version of the system is stable. It is reasonable to assume that an uncertain but stable system has bounded uncertainties.

2. The open-loop transfer function of $E_i(s)$ with respect to both $\omega_i(s)$ and $\tilde{d}(s)$ is ${\Gamma_i}^{-1}(s)$, which is a stable system matrix in the new coordinate system. Therefore, both transfer functions have real bounds.

3. The open-loop transfer function of $E_i(s)$ with respect to $\varpi_i(s)$ is a function of two factors, ${\Gamma_i}^{-1}(s)$ and a polynomial of degree r_i. This product is stable. The closed-loop transfer function is a sum of polynomials with maximum degree r_i, which cancels the term $-s^{r_i}$ and leaves a positive value K_i. Therefore, the closed-loop characteristic

polynomial has all positive coefficients, and the Hurwitz criterion implies absolute stability. This transfer function can be shown to be non-minimum phase. We know that the open-loop transfer function includes at least one zero in the right-half plane, and the closed-loop transfer function is strictly stable. Therefore, operation within the system bandwidth guarantees stability and precludes the system's root locus from moving to zero. So the transfer function from the measurement noise to the estimation error is bounded.

Condition 2 can be written as the following conditions that need to be satisfied for the boundedness of the unknown input estimation error.

$$\|\Delta_i{}^{-1}[M_{1i}\Gamma_i{}^{-1}(s)M_i + M_{4i}]\|_\infty \leq \delta p_\phi \tag{4.61}$$

$$\|\Delta_i{}^{-1}(M_{1i}\Gamma_i{}^{-1}(s)[K_i - s^{r_i}M_i] + [M_{3i} - s^{r_i}M_i - s\Psi_i])\|_\infty \leq \delta m_\phi \tag{4.62}$$

$$\|\Delta_i{}^{-1}\|_\infty \leq \eta_{d_\phi} \tag{4.63}$$

$$\|s\tilde{d}(s)\| \leq \mu \tag{4.64}$$

where δp_ϕ, δm_ϕ, η_{d_ϕ}, and μ are positive numbers that denote the upper bounds of the transfer functions from the process noise, measurement noise, unknown input derivative, and unknown input, to $\Phi_i(s)$.

The same discussion as provided above holds for each input to the unknown input estimation error dynamics. However, we have two additional parameters that contribute to the dynamics of the unknown input estimation error. These additional terms need to be addressed from the perspective of their transfer functions, magnitudes, and bounds.

Unknown input observer gain

The first additional parameter is the unknown input observer gain Ψ, which affects the transfer function from the noise to $\Phi_i(s)$, as well as the transfer function from $s\tilde{d}(s)$ to $\Phi_i(s)$. The assumption of sufficiently small noise magnitude can effectively diminish the

influence of the noise on $\Phi_i(s)$. However, to ensure good performance, we need to bound Ψ using δp_ϕ, δm_ϕ, $\|\omega_i(s)\|$, and $\|\varpi_i(s)\|$, because the transfer function from the noise to $\Phi_i(s)$ is a function of Ψ. We express bounds for Ψ as follows:

$$f_p(\Psi,s) = \frac{\Phi_i(s)}{\omega_i(s)} \leq \delta p_\phi \Rightarrow \Psi \leq \Psi_p \tag{4.65}$$

$$f_m(\Psi,s) = \frac{\Phi_i(s)}{\varpi_i(s)} \leq \delta m_\phi \Rightarrow \Psi \leq \Psi_m \tag{4.66}$$

$$f_d(\Psi,s) = \frac{\Phi_i(s)}{s\tilde{d}(s)} \leq \eta_{d_\phi} \Rightarrow \Psi \leq \Psi_d \tag{4.67}$$

where f_p, f_m, and f_d denote the transfer functions from the process noise, measurement noise, and unknown input derivative, to the unknown input estimation error. The above equations indicate that for any acceptable δp_ϕ, δm_ϕ, and η_{d_ϕ}, there exists an upper bound for Ψ defined by Ψ_p, Ψ_m, and Ψ_d. To satisfy these bounds, we take their minimum as the maximum allowable values of Ψ:

$$\Psi \leq \Psi_{max} = \min\{\Psi_p, \Psi_m, \Psi_d\} \tag{4.68}$$

Unknown input derivative

The second additional parameter is the derivative of the unknown input $s\tilde{d}(s)$, which needs to be bounded by a parameter μ for stability. This parameter plays a very important role in the stability analysis.

In the case $s\tilde{d}(s) = 0$ and a noise-free system, the estimation and control problem can be viewed as a stabilization problem. In this case, the unknown input is constant (for example, a step input), and continuity and differentiability of the unknown input are not stability requirements. Moreover, both process noise and measurement noise are still input to the system, so the system will still have steady state estimation and tracking errors.

4.7.4 Error Convergence

State estimation error

Assume that all conditions (4.61)–(4.67) related to Condition 2 are satisfied. Then the unknown input estimation error is bounded in terms of the unknown input as

$$\|\Phi(s)\| \leq [\delta_{p_\phi}]\varepsilon_p\|s\tilde{d}(s)\| + [\delta_{m_\phi}]\varepsilon_m\|s\tilde{d}(s)\| + [\eta_{d_\phi}]\|s\tilde{d}(s)\| \tag{4.69}$$

$$\|\Phi(s)\| \leq [\delta_{p_\phi}\varepsilon_p + \delta_{m_\phi}\varepsilon_m + \eta_{d_\phi}]\|s\tilde{d}(s)\| \tag{4.70}$$

Equation (4.70) shows that the unknown input estimation error is bounded in terms of $\|s\tilde{d}(s)\|$. Earlier in this chapter we saw that the input estimation error system is exponentially stable. Therefore, we can use (4.70) to write the local asymptotic exponential convergence in the time domain as

$$\|\phi(t)\| \leq \|\phi_0\|e^{-\gamma_{\phi_0}t} + \delta_{p_\phi}\varepsilon_p(1-e^{-\gamma_{p_\phi}t})\|\dot{\tilde{d}}\| + \delta_{m_\phi}\varepsilon_m(1-e^{-\gamma_{m_\phi}t})\|\dot{\tilde{d}}\| + \eta_{d_\phi}(1-e^{-\gamma_{d_\phi}t})\|\dot{\tilde{d}}\| \tag{4.71}$$

where γ_{p_ϕ}, γ_{m_ϕ}, and γ_{d_ϕ} are the roots of the transfer functions f_p, f_m, and f_d respectively. ϕ_0 denotes the initial condition of $\phi(t)$, and the γ_{ϕ_0} term comes from the roots of the transfer function ${\Delta_i}^{-1}(s)$ (the homogeneous solution of the unknown input estimation error dynamics equation). The above equation implies that

$$\lim_{t\to\infty}\|\phi(t)\| \leq [\delta_{p_\phi}\varepsilon_p + \delta_{m_\phi}\varepsilon_m + \eta_{d_\phi}]\mu \tag{4.72}$$

where μ is the upper bound of $\dot{\tilde{d}}$. We can write this as

$$\lim_{t\to\infty}\|\phi(t)\| \leq \sigma_\phi\mu \tag{4.73}$$

where $\sigma_\phi = \delta_{p_\phi}\varepsilon_p + \delta_{m_\phi}\varepsilon_m + \eta_{d_\phi}$.

Unknown input estimation error

Assume that all conditions (4.56)–(4.60) and (4.70) related to Condition 1 are satisfied. Then the state estimation error can be written as

$$\|E(s)\| \leq [\eta_{\phi_e}]\|\Phi(s)\| + [\delta_{p_e}]\varepsilon_p\|s\tilde{d}(s)\| + [\delta_{m_e}]\varepsilon_m\|s\tilde{d}(s)\| \tag{4.74}$$

$$\leq [\eta_{\phi_e}(\delta_{p_\phi}\varepsilon_p + \delta_{m_\phi}\varepsilon_m + \eta_{d_\phi}) + \delta_{p_e}\varepsilon_p + \delta_{m_e}\varepsilon_m]\|s\tilde{d}(s)\| \tag{4.75}$$

Equation (4.75) shows that the state estimation error is bounded in terms of $\|s\tilde{d}(s)\|$. Earlier in this chapter we saw that the state estimation error system is exponentially stable. Therefore, we can use (4.75) to write the local asymptotic exponential convergence in the time domain as

$$\|e(t)\| \leq \|e_0\|e^{-\gamma_{e_0}t} + \eta_{\phi_e}(\|\phi_0\|e^{-\gamma_{\phi_0}t} + \delta p_\phi\varepsilon_p(1-e^{-\gamma_{p_\phi}t})\|\dot{\tilde{d}}\| + \delta m_\phi\varepsilon_m(1-e^{-\gamma_{m_\phi}t})\|\dot{\tilde{d}}\| +$$
$$\eta_{d_\phi}(1-e^{-\gamma_{d_\phi}t})\|\dot{\tilde{d}}\|) + \delta_{p_e}\varepsilon_p(1-e^{-\gamma_{p_e}t})\|\dot{\tilde{d}}\| + \delta_{m_e}\varepsilon_m(1-e^{-\gamma_{m_e}t})\|\dot{\tilde{d}}\| \tag{4.76}$$

where γ_{p_e} and γ_{m_e} are the roots of the transfer functions from the process noise and the measurement noise to $E(s)$. e_0 denotes the initial condition of $e(t)$, and the γ_{e_0} term comes from the roots of the transfer function ${\Gamma_i}^{-1}(s)$ (the homogeneous solution of the state estimation error dynamics equation). The above equation implies that

$$\lim_{t\to\infty}\|e(t)\| \leq [\eta_{\phi_e}(\delta_{p_\phi}\varepsilon_p + \delta_{m_\phi}\varepsilon_m + \eta_{d_\phi}) + \delta_{p_e}\varepsilon_p + \delta_{m_e}\varepsilon_m]\mu \tag{4.77}$$

where μ (as before) is the upper bound of $\dot{\tilde{d}}$. We can write this as

$$\lim_{t\to\infty}\|e(t)\| \leq \sigma_e\mu \tag{4.78}$$

where $\sigma_e = \eta_{\phi_e}(\delta_{p_\phi}\varepsilon_p + \delta_{m_\phi}\varepsilon_m + \eta_{d_\phi}) + \delta_{p_e}\varepsilon_p + \delta_{m_e}\varepsilon_m$.

Discussion and Interpretation

Equation (4.77) shows that $\dot{\tilde{d}}$ plays a clear role in the unknown input estimation error, but what is the intuitive explanation of this phenomenon from the viewpoint of the physical system? Recall that $\dot{\tilde{d}}$ is the rate of change of the unknown input to the system. Depending on the rate of change, the estimation error dynamics become more or less stable. Recall the previously stated important assumption that the unknown input is smooth (continuous and differentiable). It is intuitive why this condition is key to stability and error convergence. One interesting conclusion of this analysis is that an unknown input with a large magnitude that is smooth can be rejected more effectively than an unknown input of smaller magnitude but faster dynamics.

Another point requiring discussion is the term μ, which represents the bound on the unknown input rate of change. Rate of change can be interpreted as signal bandwidth. Therefore, if we know the smallest bandwidth within which all of the system components operate, then we can set μ equal to that value. This is because, if the dynamics of the unknown input are faster than this limit, at least one of the system components will not be able to track the unknown input, and so the unknown input rate of change will be physically limited.

If the system is noise-free or the noise magnitude is negligibly small, we have $\sigma_\phi = \eta_{d_\phi}$, which implies that $\lim_{t\to\infty} \|\phi(t)\| \leq \eta_{d_\phi}\mu$, which in turn implies that

$$lim_{t\to\infty}\|e(t)\| \leq \eta_{\phi_e}\eta_{d_\phi}\mu$$

This shows the direct relationship between unknown input estimation error and state estimation error. This is intuitive and implies that a better estimation of the unknown input results in a better estimation of the states.

As shown in Chapter III, the virtual control terms v_i are independent from each other and can be selected by pole placement. This implies that v can be expressed as a

linear differential equation of the error term. On the other hand, the actual control input u_i (3.6) is a combination of v_i and $\Gamma^{-1}(x)$, the transformation matrix. Therefore, u_i can be expressed as a nonlinear differential equation of the error term. The relationship between the stability of the original nonlinear system and the transformed linear system is expressed by the following lemma [59, Chapter 3].

Lemma IV.2 *If an equilibrium point is locally (globally) exponentially stable, then it is also locally (globally) asymptotically stable. However, an equilibrium point that is locally (globally) asymptotically stable may or may not be locally (globally) exponentially stable.*

Lemma IV.2 implies that if v_i results in local exponential stability, then the actual control input u_i results in local asymptotic stability for the nonlinear dynamics.

In many engineering applications, the goal of control design is not just stabilization with respect to an equilibrium point; in this case an initial condition starting close enough to equilibrium will remain close to equilibrium. But a more difficult challenge is to return the state back to equilibrium. So a common control objective includes both stabilization and asymptotic convergence. As an example, consider a satellite that has been subjected to a disturbance. Two tasks need to be addressed: keeping the satellite state in a bounded range that is determined by the magnitude of the disturbance, and returning the satellite state to equilibrium. Recall from the beginning of Section 4.2 when we discussed stability types that the region or domain of attraction is crucial for attaining asymptotic stability. However, defining or computing these regions are extremely difficult [59, Chapter 3]. But in many cases we can at least obtain an estimate of the domain of attraction, even if the estimate may be conservative.

Let us make a conservative estimate of the attraction domain in our robot / prosthesis system. Assume that the region is bounded by μ, meaning that every trajectory starting in this region will eventually converge to the final bound $\sigma_e\mu$. This assumption implies that the final bound is less than μ. Otherwise, there will not be asymptotic convergence. In general, it is reasonable to bound or limit the region of attraction with an upper

bound of the unknown input derivative. The parameter μ is thus a key factor in the dynamics of both the state estimation and the unknown input estimation, as well as a physical property of the system.

4.7.5 Local Asymptotic Stability

Based on the previous discussion, the conditions, and the bounds, we now proceed to introduce a theorem and its proof to highlight and conclude this chapter. Recall that the robot's dynamic model in affine state space form with unknown inputs is written as (3.12)

$$\dot{x} = f(x,t) + g(x,t)u + \varpi(t) + E(x,t)\,d(x,t)$$

$$y = h(x,t) + \varpi(t) \tag{4.79}$$

where $d(x,t) \in \mathbb{R}^l$ is the unknown input vector, and $E(x,t)\,d(x,t)$ comprises the effect of the unknown inputs on each joint. The m decoupled subsystems that result from the linearization transformation are given as

$$\begin{aligned} \dot{Z}_1^i(t) &= Z_2^i(t) \\ &\vdots \\ \dot{Z}_{r_i}^i(t) &= y_i^{(r_i)}(t) = v_i(t) + \gamma_i(t) + \tilde{d}_i(x,t) \end{aligned} \tag{4.80}$$

for $i = 1,2,\ldots,m$. The virtual control input (3.15) that satisfies Hurwitz stability is given as

$$v_i(t) = Z_{di}^{(r_i)}(t) - \theta_i^T e_i(t) - \hat{\tilde{d}}_i(x,t) \tag{4.81}$$

where the gain matrix $\theta_i^T = \left[\theta_{r_i}^i, \cdots, \theta_1^i\right]$ is designed by pole placement to provide a Hurwitz polynomial $e_i^{(r_i)} + \theta_1^i e_i^{r_i-1} + \ldots + \theta_{ri}^i e_i$, where the state estimation error $e_i(t) = \hat{Z}_i - Z_{di}$.

Theorem IV.8 *Suppose that the system* (4.79) *has total relative degree r and that its zero dynamics are locally asymptotically stable. Suppose that we design unknown input observers and compensators with gains* Ψ_i *for each of the i subsystems* (4.80)*. Then the control inputs* u_i *result in a locally asymptotically stable closed-loop system that is robust in the presence of disturbances and unknown inputs.*

Proof. Each subsystem with relative degree $r_i = 0$ has no internal dynamics and thus is stable, meaning that all of the states remain bounded during tracking. For each subsystem with relative degree $r_i > 0$, substitute (4.81) into (4.80) to obtain

$$\dot{Z}^i_{r_i}(t) = Z^{(r_i)}_{di}(t) - \theta_i^T e_i(t) - \hat{\tilde{d}}_i(x,t) + \gamma_i(t) + \tilde{d}_i(x,t) \tag{4.82}$$

$$\underbrace{\dot{Z}^i_{r_i}(t) - Z^{(r_i)}_{di}(t) + \theta_i^T e_i(t)}_{\text{state estimation error } e_i(t)} + \underbrace{\hat{\tilde{d}}_i(x,t) - \tilde{d}_i(x,t)}_{\text{unknown input estimation error } \phi_i(t)} - \gamma_i(t) = 0 \tag{4.83}$$

Equations (4.73) and (4.78) have shown that these two errors are bounded and can be designed to converge to any desired positive value, assuming that the magnitudes of the noise terms are sufficiently small. Consequently, the closed-loop dynamics is locally exponentially stable when the virtual control input v is applied to the linearized dynamics, and locally asymptotically stable when the actual control input u is applied to the nonlinear dynamics. ■

In the case of internal or zero dynamics, the Lyapunov linearization method provides a straightforward approach to explore stability. The theorem suggests using a Taylor series expansion around the equilibrium point to neglect terms higher than first order, and then constructing an augmented system matrix to allow a stability investigation of the full closed-loop system.

4.8 Discussion

We discussed Lyapunov stability types and then discussed theorems to extend the concept of stability to both linear and nonlinear systems. We provided a systematic proof of the stability of the proposed derivative-free Kalman filter (DKF) for state estimation of a closed-loop robotic system with noise and unknown inputs. We analyzed the error dynamics in both frequency and time domain, and derived the conditions for the convergence of these errors. Finally, we provided a theorem to show that the DKF-based system dynamics is locally asymptotically stable.

CHAPTER V

CONCLUSION AND FUTURE WORK

5.1 Conclusion

This thesis first provided an introduction to nonlinear control systems. It highlighted the importance of nonlinear control design and introduced various types and aspects of system nonlinearity. Two primary objectives of nonlinear control design (stabilization and trajectory tracking) were discussed. Common nonlinear control methods were briefly introduced. Feedback linearization was introduced as a technique for nonlinear control design and system transformation. Input state linearization in conjunction with a standard Kalman filter (that is, estimation-based control) was discussed. An example of DC-servo position control as a nonlinear SISO control problem was introduced to demonstrate the effectiveness of estimation-based feedback linearization control.

The thesis extended the idea of linearization with feedback linearization for MIMO systems. It introduced input-output linearization for a class of nonlinear systems. Robot dynamics were considered as a highly nonlinear system that could be controlled with input-output linearization. To provide estimation-based control, the linearized model was subjected to a standard Kalman filter for state estimation, which is known as the derivative-free Kalman filter (DKF). A three-DOF robot / prosthesis system was considered as an example of an MIMO system that was disturbed by noise and unknown ground reaction force (that

is, unknown external input). PI and PD methods were introduced as supervisory control terms to make the system dynamics robust to the unknown input.

The thesis systematically analyzed the stability of the DKF-based closed-loop system. It began with a short introduction to the concept of stability for nonlinear systems. Lyapunov theorems and invariant set theorems were introduced as two powerful methods to address stability in nonlinear systems. Lyapunov-based stability analysis of linear systems, along with stability analysis of non-autonomous systems, or time-varying systems, was also discussed.

A stability analysis of the DKF-based control method was presented. The dynamics of both the state estimation error and the unknown input estimation error was constructed. The Laplace transform of the dynamics provided an opportunity for a frequency-domain analysis of both errors. The transformation allowed the treatment of noise and its derivatives as a single unit. It also allowed the application of superposition theory to determine the influence of all inputs on the error dynamics. The transfer function approach allowed the evaluation of the relative importance of each input on the error dynamics.

Assumptions and bounds for the system inputs and their transfer functions were introduced and justified. Every real-world system includes assumptions and bounds that should be considered before or during control design. In order to obtain stable, reliable, and desired performance, control system designers must recognize the system's limitations and account for the limitations in such a way as to achieve desirable operation in the presence of constraints. Conditions related to the boundedness of both state estimation error and input estimation error were addressed.

It was seen that the derivative of the unknown input plays an important role in the dynamics of both the state estimation error and the input estimation error. This led us to examine this term as a special factor in the DKF-based control system. It was shown that this factor is strongly related to the region of attraction for local asymptotic stability, and also to the unknown input estimator gain. The thesis discussed approaches for defining the

region of attraction and the estimator gain.

Finally, the thesis introduced a theorem and proof to address the stability of the closed-loop estimation-based control system. It was shown that the error dynamics of the linearized model with virtual control is locally exponentially stable and that the error thus converges to a finite bound as time tends to infinity. This implies that the actual control provides local asymptotic stability for the nonlinear robot / prosthesis system.

5.2 Future Work

One interesting topic of recent research is simultaneous estimation of both states and unknown inputs. This topic has received more attention as researchers have observed that information about unknown inputs is a key factor for both improved state estimation and closed-loop system stability. We see potential advantages to using an observer for unknown input estimation rather than simply using a PD or PI supervisory control term. This would provide the observer with a dynamic gain as opposed to a constant gain, which in turn could improve performance, adaptability, and stability.

Another interesting idea for future work is to obtain quantitative results for the stability conditions in this thesis. The system could be tested under with various initial conditions and unknown inputs to numerically evaluate error convergence or divergence.

Practical implementation of these results would be another interesting direction for future research. This could help verify the simulation results.

Finally, the DKF-based feedback linearization control method could be explored for other systems. This could show the effectiveness of the method in different areas and demonstrate the method's flexibility. Potential applications could be quite diverse, including biology, economics, meteorology, and others. The only limitation is that the system needs to be linearizable; in other words, its dynamics need to be expressed in affine state space form.

BIBLIOGRAPHY

[1] P. F. Adams, G. E. Hendershot, and M. A. Marano. Current estimates from the national health interview survey. Centers for Disease Control and Prevention/National Center for Health Statistics, 10(200):1–203, 1996.

[2] S. K. Au and H. Herr. Powered ankle-foot prosthesis for the improvement of amputee ambulation. In 29th Annual IEEE Conference Engineering in Medicine and Biology Society, pages 3020–3026, Lyon, France, 2007.

[3] S. K. Au and H. Herr. Powered ankle foot prosthesis. IEEE Robotics and Automation Magazine, 15(3):52–59, 2008.

[4] S. K Au and J. Weber. Biomechanical design of a powered anklefoot prosthesis. In IEEE International Conference on Rehabilitation Robotics, pages 298–303, Noordwijk, Netherlands, 2007.

[5] V. Azimi, D. Simon, and H. Richter. Stable robust adaptive impedance control of a prosthetic leg. In ASME Dynamic Systems and Control Conference, Columbus, Ohio, 2015.

[6] V. Azimi, D. Simon, H. Richter, and S. A. Fakoorian. Robust composite adaptive transfemoral prosthesis control with non-scalar boundary layer trajectories. In American Control Conference, Boston, Massachusetts, 2016.

[7] G. Basile and G. Marro. On the observability of linear, time-invariant systems with unknown inputs. Journal of Optimization Theory and Applications, 2(6):410–415, 1969.

[8] S. Bolognani, R. Oboe, and M. Zigliotto. Sensorless full-digital PMSM drive with EKF estimation of speed and rotor position. IEEE Transactions on Industrial Electronics, 46(1):184–191, 1999.

[9] J. Chen, R. Patton, and H. Zhang. A class of extended state observers for uncertain systems. Control and Decision, 10(1):85–88, 1995.

[10] J. Chen, R. Patton, and H. Zhang. Design of unknown input observers and robust fault detection filters. International Journal of Control, 63(1):85–105, 1995.

[11] Y. Cheng, H. Ye, Y. Wang, and D. Zhou. Unbiased minimum-variance state estimation for linear systems with unknown input. Automatica, 45(2):485–491, 2009.

[12] T. Chin, S. Sawamura, R. Shiba, H. Oyabu, Y. Nagakura, and A. Nakagawa. Energy expenditure during walking in amputees after disarticulation of the hip. Journal of Bone and Joint Surgery, 87(1):117–119, 2005.

[13] M. Corless and J. Tu. State and input estimation for a class of uncertain systems. Automatica, 34(6):757–764, 1998.

[14] J. M. Czerniecki, A. Gitter, and C. Munro. Joint moment and muscle power output characteristics of below knee amputees during running: the influence of energy storing prosthetic feet. Journal of Biomechanics, 24(1):63–75, 1991.

[15] M. Darouach and M. Zasadzinski. Unbiased minimum variance estimation for systems with unknown exogenous inputs. Automatica, 33(4):717–719, 1997.

[16] D. Ebeigbe, D. Simon, and H. Richter. Hybrid function approximation based control with application to prosthetic legs. In IEEE International Systems Conference, pages 111–116, Orlando, Florida, 2016.

[17] S. Fakoorian. Ground reaction force estimation in prosthestic legs with an extended Kalman filter. Master's thesis, Cleveland State University, Cleveland, OH, 2016.

[18] S. A. Fakoorian, V. Azimi, S. M. Moosavi, H. Richter, and D. Simon. Ground reaction force estimation in prosthetic legs with nonlinear Kalman filtering methods. ASME Journal of Dynamic Systems, Measurement, and Control, 139(11):111004, 2017.

[19] S. A. Fakoorian, D. Simon, H. Richter, and V. Azimi. Ground reaction force estimation in prosthetic legs with an extended Kalman filter. In IEEE International Systems Conference, pages 338–343, Orlando, Florida, 2016.

[20] Z. Gao. Active disturbance rejection control: A paradigm shift in feedback control system design. In American Control Conference, 2006.

[21] Z. Gao, S. Hu, and F. Jiang. A novel motion control design approach based on active disturbance rejection. In IEEE Conference on Decision and Control, page 4974, 2001.

[22] S. Gillijns and B. De Moor. Unbiased minimum-variance input and state estimation for linear discrete-time systems with direct feedthrough. Automatica, 43(5):934–937, 2007.

[23] V. Gourishangkar, P. Kudva, and K. Ramar. Reduced-order observers for multivariable systems with inaccessible disturbance inputs. International Journal of Control, 25(4):311–319, 1977.

[24] R. Gregg, T. Lenzi, L. Hargrove, and J. Sensinger. Virtual constraint control of a powered prosthetic leg: From simulation to experiments with transfemoral amputees. IEEE Transactions on Robotics, 30(6):1455–1471, 2014.

[25] R. Gregg, T. Lenzi, L. Hargrove, and J. Sensinger. Virtual constraint control of a powered prosthetic leg: from simulation to experiments with transfemoral amputees. IEEE Transactions on Robotics, 30(6):1455–1471, 2014.

[26] R. Gregg and J. Sensinger. Towards biomimetic virtual constraint control of a powered prosthetic leg. IEEE Transactions on Control System Technology, 22(1):246–254, 2014.

[27] L. Guo and W. H. Chen. Disturbance attenuation and rejection for systems with nonlinearity via DOBC approach. International Journal of Robust and Nonlinear Control, 15(3):109–125, 2005.

[28] Z. Harvey, B. Potter, J. Vandersea, and E. Wolf. Prosthetic advances. Journal of Surgical Orthopaedic Advances, 21(1):58–64, 2012.

[29] Y. Hori, K. Shimura, and M. Tomizuka. Position/force control of multi-axis robot manipulator based on the TDOF robust servo controller for each joint. In American Control Conference, pages 753–757, 1992.

[30] G. H. Hostetter and J. Meditch. On the generalization of observers to systems with unmeasurable, unknown inputs. Automatica, 9(4):721–724, 1973.

[31] Y. Hou, Z. Gao, F. Jiang, and B. Boulter. Active disturbance rejection control for web tension regulation. In IEEE Conference on Decision and Control, 2001.

[32] J. Johansson, D. Sherrill, P. Riley, P. Bonato, and H. Herr. A clinical comparison of variable-damping and mechanically passive prosthetic knee devices. American Journal of Physical Medicine and Rehabilitation, 84(8):563–575, 2005.

[33] C. Johnson. Accommodation of external disturbances in linear regulator and servomechanism problems. IEEE Transactions on Automatic Control, AC-16(6):635–644, 1971.

[34] G. Khademi, H. Mohammadi, E. C. Hardin, and D. Simon. Evolutionary optimization of user intent recognition for transfemoral amputees. In Biomedical Circuits and Systems Conference, pages 1–4, Atlanta, Georgia, 2015.

[35] P. Kitanidis. Unbiased minimum-variance linear state estimation. Automatica, 23(6):775–778, 1987.

[36] S. Kwon and W. Chung. Combined synthesis of state estimator and perturbation observer. ASME Journal of Dynamic Systems, Measurement, and Control, 125(4):19–26, 2003.

[37] S. Kwon and W. Chung. A discrete-time design and analysis of perturbation observer for motion control applications. IEEE Transactions on Automatic Control, 11(3):399–407, 2003.

[38] B. Lambrecht and H. Kazerooni. Design of a semi-active knee prosthesis. In IEEE Conference on Robotics and Automation, pages 639–645, 2009.

[39] M. Liu, D. Wang, and H. Huang. Development of an environment-aware locomotion mode recognition system for powered lower limb prostheses. IEEE Transactions on Neural Systems and Rehabilitation Engineering, 24(4):434–443, 2016.

[40] Y. Liu and D. Söffker. Robust control approach for inputoutput linearizable nonlinear systems using high-gain disturbance observer. International Journal of Robust and Nonlinear Control, 24(2):326–339, 2014.

[41] C. Martinez, J. Weber, G. Elliott, and H. Herr. Design of an agonist-antagonist active knee prosthesis. In International Conference on Biomedical Robotics and Biomechatronics, pages 529–534, Scottsdale, AZ, 2008.

[42] H. Mohammadi and H. Richter. Robust tracking/impedance control: application to prosthetics. In American Control Conference, pages 2673–2678, Chicago, Illinois, 2015.

[43] S. M. Moosavi, S. A. Fakoorian, V. Azimi, H. Richter, and D. Simon. Derivative-free Kalman filtering-based control of prosthetic legs. In American Control Conference, Seattle, Washington, 2017.

[44] P. C. Müller. Indirect measurements of nonlinear effects by state observers. IUTAB Symposium on Nonlinear Dynamics in Engineering Systems, pages 205–215, 1990.

[45] G. De Nicolao, G. Sparacino, and C. Cobelli. Nonparametric input estimation in physiological systems: Problems, methods, and case studies. Automatica, 33(5):851–870, 1997.

[46] K. Norton. A brief history of prosthetics. Amputee Coalition, 17(7):pp, 2007.

[47] R. Patton, R. Clark, and P. Frank. Fault diagnosis in dynamic systems: theory and applications. Prentice Hall, 1989.

[48] A. Rashvand. Exploratory particle swarm optimization: Stability and robot control tuning. Master's thesis, Cleveland State University, Cleveland, OH, 2015.

[49] E. C. Rasmussen and C. K. I. Williams. Gaussian Processes for Machine Learning. MIT press, 2006.

[50] H. Richter and D. Simon. Robust tracking control of a prosthesis test robot. ASME Journal of Dynamic Systems, Measurement, and Control, 136(3):031011, 2014.

[51] H. Richter, D. Simon, W. Smith, and S. Samorezov. Dynamic modeling, parameter estimation and control of a leg prosthesis test robot. Applied Mathematical Modelling, 39(12):559–573, 2015.

[52] G. G. Rigatos. A derivative-free Kalman filtering to state estimation-based control of a class of nonlinear system. IEEE Transactions on Industrial Electronics, 59(10):3987–3997, 2012.

[53] G. G. Rigatos. Nonlinear Control and Filtering Using Differential Flatness Approaches: Applications to Electromechanical Systems. Springer, 2015.

[54] F. Schlaepfer and F. Schweppe. Continuous-time state estimation under disturbances bounded by convex sets. IEEE Transactions on Automatic Control, 17(2):197–205, 1972.

[55] E. Schrijver and J. van Dijk. Disturbance observers for rigid mechanical systems: Equivalence, stability, and design. ASME Journal of Dynamic Systems, Measurement, and Control, 124(4):539–548, 2002.

[56] A. Segal, M. Orendur, G. Klute, and M. L. McDowell. Kinematic and kinetic comparisons of transfemoral amputee gait using C-leg and Mauch SNS prosthetic knees. Journal of Rehabilitation Research and Development, 43(7):857–870, 2006.

[57] Y. S. Shmaliy. An iterative Kalman-like algorithm ignoring noise and initial conditions. IEEE Transactions on Signal Processing, 59(6):2465–2473, 2011.

[58] D. Simon. Optimal State Estimation: Kalman, H-Infinity, and Nonlinear Approaches. John Wiley & Sons, 2006.

[59] J.-J. Slotine and W. Li. Applied Nonlinear Control. Prentice-Hall, 1991.

[60] D. Söffker, T.-J. Yu, and P. Müller. State estimation of dynamical systems with nonlinearities by using proportional-integral observer. International Journal of Systems Science, 26(9):1571–1582, 1995.

[61] B. Sun and Z. Gao. A DSP-based active disturbance rejection control design for a 1 KW H-bridge DC-DC power converter. IEEE Transactions on Industrial Electronics, 52(5):1271–1277, 2005.

[62] F. Sup, H. Varol, J. Mitchell, and T. Withrow. Preliminary evaluations of a self-contained anthropomorphic transfemoral prosthesis. IEEE Transactions on Mechatronics, 14(6):667–676, 2009.

[63] F. Sup and H. A. Varol. Upslope walking with a powered knee and ankle prosthesis: Initial results with an amputee subject. IEEE Transactions on Neural Systems and Rehabilitation Engineering, 19(1):71–78, 2010.

[64] T. Umeno and Y. Hori. Robust speed control of DC servomotors using modern two degrees-of-freedom controller design. IEEE Transactions on Industrial Electronics, 38(5):363–368, 1991.

[65] Y. Wen, J. Si, X. Gao, S. Huang, and H. Huang. A new powered lower limb prosthesis control framework based on adaptive dynamic programming. IEEE Transactions on Neural Networks and Learning Systems, 2017.

[66] S. Yong, M. Zhu, and E. Frazzoli. Simultaneous input and state estimation for linear discrete-time stochastic systems with direct feedthrough. In IEEE Conference on Decision and Control, pages 485–491, 2009.

[67] S. Yong, M. Zhu, and E. Frazzoli. Simultaneous input and state estimation for linear time-varying continuous-time stochastic systems. IEEE Transactions on Automatic Control, 62(5):2531–2538, 2017.

[68] A. J. Young, A. M. Simon, and L. J. Hargrove. A training method for locomotion mode prediction using powered lower limb prostheses. IEEE Transactions on Neural Systems and Rehabilitation Engineering, 22(3):671–677, 2014.

[69] H. Zhao, J. Horn, J. Reher, and A. Ames. Multi-contact locomotion on transfemoral prostheses via hybrid system models and optimization-based control. IEEE Transactions on Automation Science and Engineering, 13(2):502–513, 2016.

[70] H. Zhao, S. Kolathaya, and A. D. Ames. Quadratic programming and impedance control for transfemoral prosthesis. In International Conference on Robotics and Automation, pages 1341–1347, Hong Kong, 2014.

[71] K. Ziegler-Graham. Estimating the prevalence of limb loss in the United States: 2005 to 2050. Archives of Physical Medicine and Rehabilitation,, 89(3):422–429, 2008.

APPENDIX

APPENDIX A

The Robot / Prosthesis System Matrices and Parameters

The dynamic equation of the robot / prosthesis system of (3.1) is repeated here for ease of reference:

$$\begin{aligned} u - J_e{}^T F_e &= M(q)\ddot{q} + C(q,\dot{q})\dot{q} + G(q) \\ &= Y(q,\dot{q},\ddot{q})\Theta \end{aligned}$$

where $Y(q,\dot{q},\ddot{q})$ is the regressor matrix and Θ is the parameter vector. The effect of the GRF on the generalized joint torques, $J_e^T F_e$, is given in (3.21). The system parameters can be written in terms of Θ as follows [5], [50].

$\Theta_1 = m_1 + m_2 + m_3$

$\Theta_2 = m_3 l_2 + m_2 l_2 + m_2 c_2$

$\Theta_3 = c_3 m_3$

$\Theta_4 = I_{2z} + I_{3z} + c_2^2 m_2 + c_3^2 m_3 + l_2^2 m_2 + l_2^2 m_3 + 2c_2 l_2 m_2$

$\Theta_5 = l_2 m_3 c_3$

$\Theta_6 = m_3 c_3^2 + I_{3z}$

$$\Theta_7 = b$$

$$\Theta_8 = f$$

$$M(1,1) = \Theta_1$$

$$M(1,2) = \Theta_3 \cos(q_3 + q_2) + \Theta_2 \cos(q_2)$$

$$M(1,3) = \Theta_3 \cos(q_3 + q_2)$$

$$M(2,1) = M(1,2)$$

$$M(2,2) = \Theta_4 + 2\Theta_5 \cos(q_3)$$

$$M(2,3) = \Theta_6 + \Theta_5 \cos(q_3)$$

$$M(3,1) = M(1,3)$$

$$M(3,2) = M(2,3)$$

$$M(3,3) = \Theta_6$$

$$C(1,1) = 0$$

$$C(1,2) = -\dot{q}_2 \left(\Theta_3 \sin(q_2 + q_3) + \Theta_2 \sin(q_2)\right) - \dot{q}_3 \Theta_3 \sin(q_2 + q_3)$$

$$C(1,3) = -\dot{q}_2 \Theta_3 \sin(q_3 + q_2) - \dot{q}_3 \Theta_3 \sin(q_3 + q_2)$$

$$C(2,1) = 0$$

$$C(2,2) = -\dot{q}_3 \Theta_5 \sin(q_3)$$

$$C(2,3) = -\dot{q}_2 \Theta_5 \sin(q_3) - \dot{q}_3 \Theta_5 \sin(q_3)$$

$$C(3,1) = 0$$

$$C(3,2) = \dot{q}_2 \Theta_5 \sin(q_3)$$

$$C(3,3) = 0$$

$$G(1) = -g\Theta_1$$

$$G(2) = -g\left(\Theta_2 \cos(q_2) + \Theta_3 \cos(q_3 + q_2)\right)$$

$$G(3) = -g\Theta_3 \cos(q_3 + q_2)$$

The system parameters are defined in Table II.

Table II: Parameters used in the robot/prosthesis system

Parameter	**Symbol**	**Value**	**Units**
Mass of link 1	m_1	40.59	kg
Mass of link 2	m_2	8.57	kg
Mass of link 3	m_3	2.29	kg
Length of link 2	l_2	0.43	m
Length of link 3	l_3	0.53	m
Distance joint 1 to link 2	c_2	0.09	m
Distance joint 2 to link 3	c_3	0.32	m
Rotary inertia of link 2	I_{2z}	0.43	kg-m^2
Rotary inertia of link 3	I_{3z}	0.06	kg-m^2
Link 1 sliding friction	f	83.33	N
Link 2 rotary damping	b	9.75	N-m-s
Acceleration due to gravity	g	9.81	m/s^2